多電極液晶透鏡(MeDLC lens) 應用在 2D/3D 轉換影像之設計

碩士研究生：沈拓江　　指導教授：謝漢萍教授
　　　　　　　　　　　　　　　黃乙白助理教授

國立交通大學　　　光電工程研究所

摘　　要

為了得到更自然的立體影像,近年來已吸引許多專家及廠商投入立體顯示器的發展。藉由對影像融入視覺上的深度,這些技術讓消費者更能感知到更真實的立體效果。對於不需配戴眼鏡的 3D 顯示器來說,需要固定式的光學元件例如:視差遮罩或柱狀透鏡。然而絕大多數顯示器皆應用於 2D 影像顯示,增加這些額外 3D 光學元件,會造成 2D 影像品質的降低。

為了能有 3D 影像且維持 2D 影像品質,可藉由轉換光學元件來造成光路徑的更改,藉此便能達成 2D 與 3D 影像間高自由度的切換。本論文設計出能自由切換於 2D 影像與 3D 影像的光學元件(MeDLC),針對其聚焦能力做了評估,以降低其影像間互相干擾的效果,進而提升立體顯示之影像品質與效率。

模擬中,設計出其最佳結構,並達到理想曲線。實作上,可達到近乎完美的理想曲線。從量測結果 MeDLC 在 beam size 上比傳統雙電極液晶透鏡小了 35%,數值孔徑分析中 MeDLC 也較傳統的高出了 66%,再者,電壓的需求也較為的低。因此,在 crosstalk 影響的程度上,比傳統透鏡降低了約 43%。

Autostereoscopic 2D/3D Switching Display with Multi-Electrically Driven Cylindrical Liquid Crystal Lens (MeDLC)

Student: To-Chiang Shen   Advisor: Dr. Han-Ping D. Shieh

Dr. Yi-Pai Huang

Institute of Electro-Optical Engineering
National Chiao Tung University

Abstract

In order to get more natural 3D sensation from displays, many researchers and manufacturers were attracted to invest in the development of 3D display technology in recent years. These technologies make it possible for the users to obtain more immersive experience by adding the real depth to the visual content shown on the display. In the case of non-glasses lenticular lens sheets must be prepared. However, since most of display applications have majority in displaying 2D image content, the fixed optical elements used for the 3D modes cause the degradation of the displayed 2D image quality.

To overcome the degradation of 2D image quality under a given 3D displays, optical paths must be controlled by switching the optical elements to change 2D and 3D modes. In this thesis we designed an optical component that can switched between 2D and 3D images, and estimate the focusing capability to reduce the effect of crosstalk. So that can enhance the image quality of 3D images.

In the simulation results, an optimized structure was designed to fit the lens-like distribution. The lens-like distribution has vivid improved compared to that of conventional double electrode LC lens. In experiment, the lens-like distribution was achieved as well. The measurement result also indicates that our device is closer to the ideal lens-like distribution. And the numerical aperture (NA) of our device shows an improve by a factor of 1.66. Also the voltage requirement is much lower with same NA. In addition, due to a smaller beam size of proposed design the crosstalk of our device is lower than that of the conventional double electrode LC lens about 43%. In conclusion, the 3D displays with proposed method not only smaller beam size and lower crosstalk, but lower operation voltage.

誌　　謝

Table of Contents

Figure Captions

List of Tables

Chapter 1

Introduction

1.1 Preface

Display technologies have been developed for over a hundred years as shown in Fig. 1-1. K.F. Braun invented the cathode ray tube (CRT) in 1897. Thereafter displays progress changed from black and white to colorful cathode ray tubes (CRTs). Afterward flat panel was invented and used widely because CRTs were bulky. In order to satisfy human visual pleasure many researchers have focused on high-definition televisions (HDTVs). All previous effort had given us more realistic image. However, the image quality isn't as real as the real world due to two-dimensional images expression. Thus the techniques above are used for 2D displays.

| Black & White TV | CRT | Flat Panel Display | HDTV | 3D Display |

| 1925 | 1950 | 1975 | 1995 | 2000 |

Fig. 1-1 History of display technology

The developments of display were motivated by trying to realize the image appears more natural. The 3D display has caught the most affection. Because of the complex sensitivity to human vision. In order to get more natural 3D images from displays, 3D display technologies are expected to be the dominant display of the next generation.

1.2 Principle of 3D image

The main mechanism for seeing 3D is the viewpoint dependent disparity between the images seen by each eye. These images will converge in our brain to give a sensation of depth by a process known as *stereopsis* [1] [2]. Sense of depth and motion are independent systems that are used to judge the distance and speed. In real world there are more than one depth cue that is available for us. Majorly speaking depth cues can be divided into two parts : visual cue, and oculomotor cue. And for the visual cue can also be divide into two different kids: monocular depth cues , binocular depth cues, as shown in Fig. 1-2 [3].
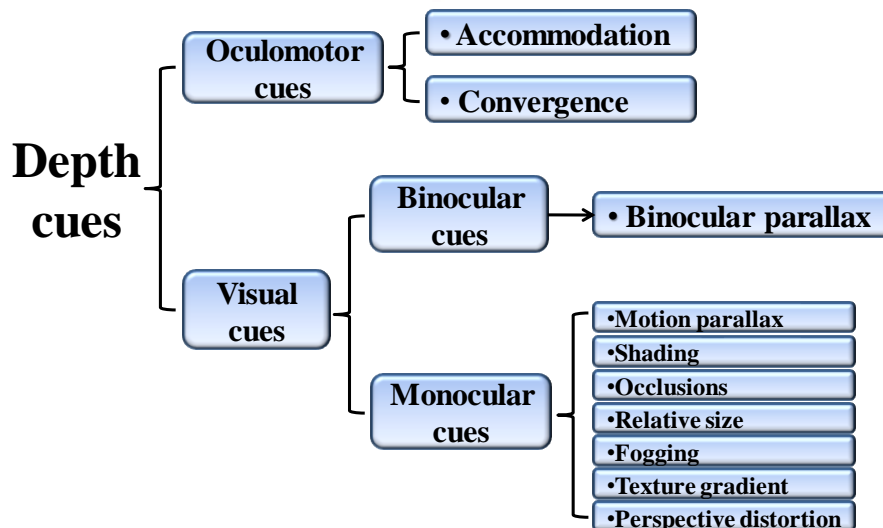
Fig. 1-2 Depth cues. [3]

Accommodation

The change of shape performed by the eye lens to focus on an object aids the brain in determining the object's distance as shown in Fig. 1-3. But this only effect in short distance (~3m).

Thick lens – object is near

Thin lens – object is near
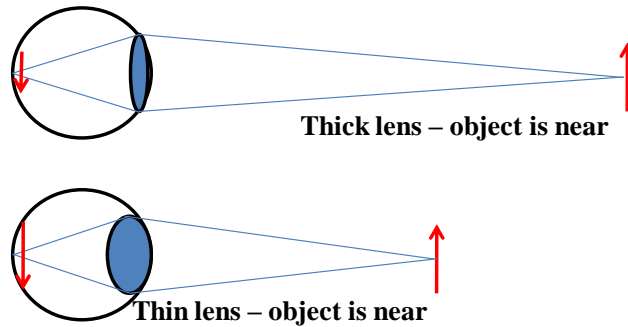
Fig. 1-3 Accommodation

Convergence

The angle between the lines of slight of each eye is larger as an object moves closer, and that only works with nearby objects (~20m) as shown in Fig. 1-4.
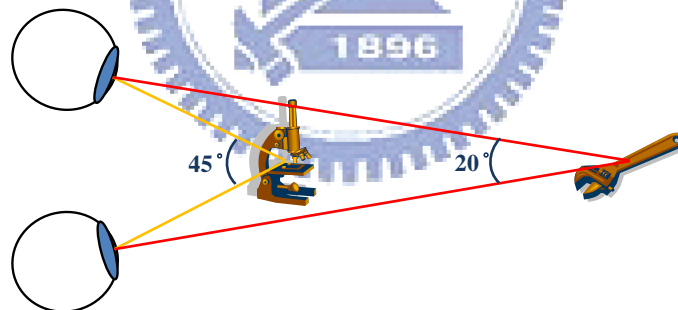
Fig. 1-4 Convergence

Binocular parallax

Each eye receives slightly different views of a scene. The two views are used to determine the ratio of distances between nearby objects. Because according to the statistics the average distance between each eye is approximately 6.5cm. Thus cause the imaging on the retinas to have a slightly different. In this case human brain can combine these images to produce a strong perception of depth as showing in Fig. 1-5.

3
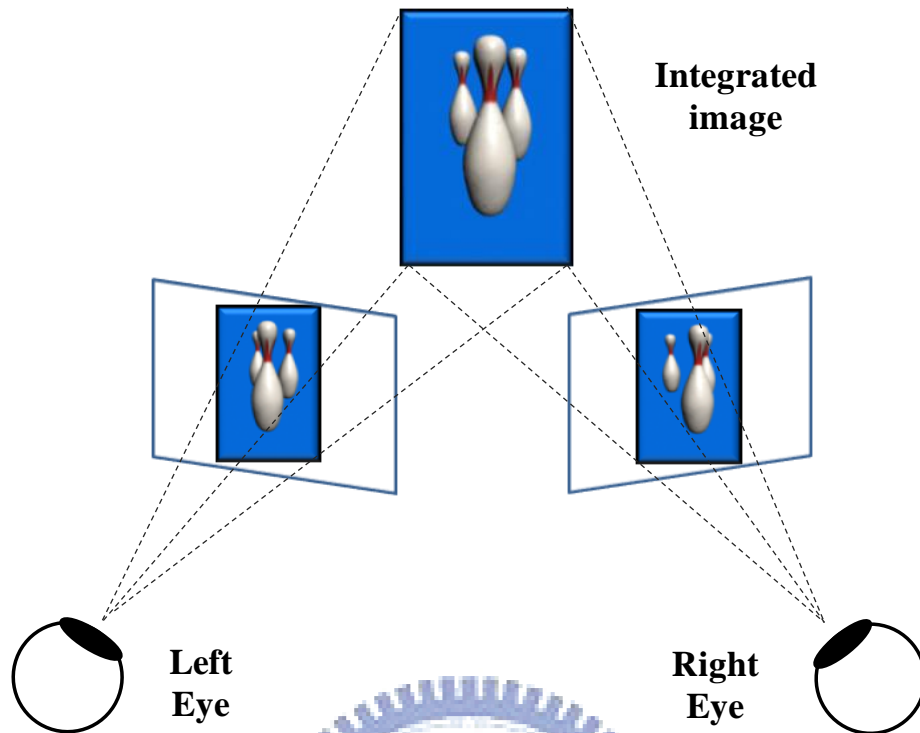
Fig. 1-5 Binocular parallax

Motion parallax

Motion parallax is a depth cue that results from our motion. As we move, objects that are closer to us move farther across our field of view than do objects that are in the distance.

Others

Beside motion parallax there are still many other cues that can provide a sense of depth. And all of those are the basic cues of how human perceive 3D image.

In the real world, human can easily perceive the depth information by using the cues that mentioned above. However in the display system it cannot produce 3D information by the occulomotor cues (convergence and accommodation). Therefore, in 3D display system have to use beside occulomotor cues.

1.3 3D display technologies

Generally, 3D display can be divided into two parts which are Stereoscopic and Auto-stereoscopic (with and without glasses) as shown in Fig. 1-6. For different application can be suitable for different field such as entertainment, personal, medical, public, military etc.
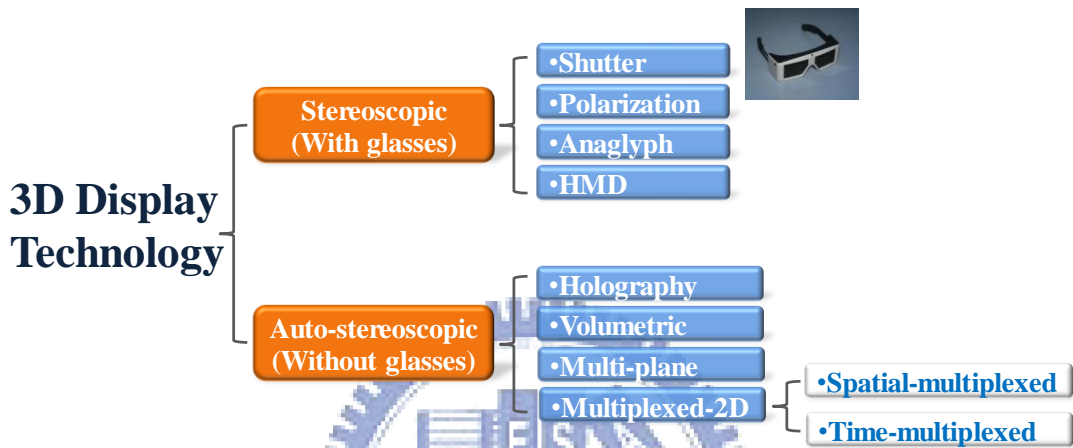
Fig. 1-6 Classification of 3D display technology

1.3.1 Stereoscopic

3D displays which require glasses to provide different views for the left and right eye also make ensure image are seen by correct eye. For example: shutter glasses divide the image into odd and even images. And if odd images are for the right eye than simultaneously the left eye is covered and vice versa. This method allowed humans to perceive 3D images. However, these glasses are costly and viewers need to wear a device.

1.3.2 Auto-stereoscopic

For the auto-stereoscopic that are viewers don't need to wear any devices and can perceive 3D images with the naked eye. There are various kinds of technologies that can produce 3D images, such as the holographic type [4], volumetric type [5], multi-plane type, and multiplexed-2D type. The previous three techniques produce 3D images directly as seen in the real world. But they have drawbacks such as: the holographic type is hard to produce on a large scale, the volumetric type is too bulky, and the multi-plane type has an alignment issue and can only view the image from a single front angle of the display.

For the past few years the most popular method adopted by researchers is providing different images to both eyes from different viewing angles using the same display system. This is because the human brain can integrate images from both eyes to become a stereoscopic image. This is also known as the "multiplexed-2D type", and can be divided into two parts: spatial-multiplexed and time-multiplexed.
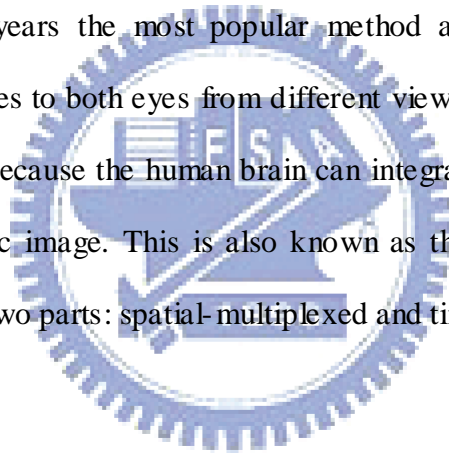
1.3.3 Multiplexed-2D type displays

The general idea of spatial-multiplexed and time-multiplexed is as shown in Fig. 1-7. The spatial-multiplexed is to divide the image into left and right image then project the image to both eyes individually. But the time-multiplexed is to provide the left and right image sequentially. These multiplexed systems all require optical component and liquid crystal displays (LCDs) to project the image to left and right eye.

Spatial-multiplexed
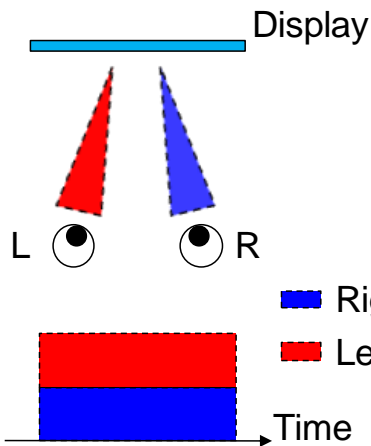
Time-multiplexed
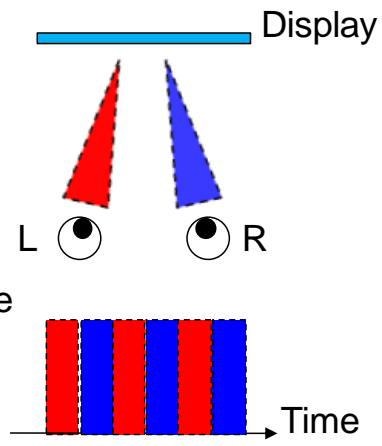
Fig. 1-7 General idea of the spatial and time multiplexed type.

There are many kinds of optical configuration of time-multiplexed have been proposed [6] [7] [8]. One idea is use the principle of total internal reflection (TIR) to reflect the light to certain direction, as shown in Fig. 1-8 [9]. By switching two light sources sequentially can make the light to reflect to certain direction. Therefore the 3D image can be perceived.
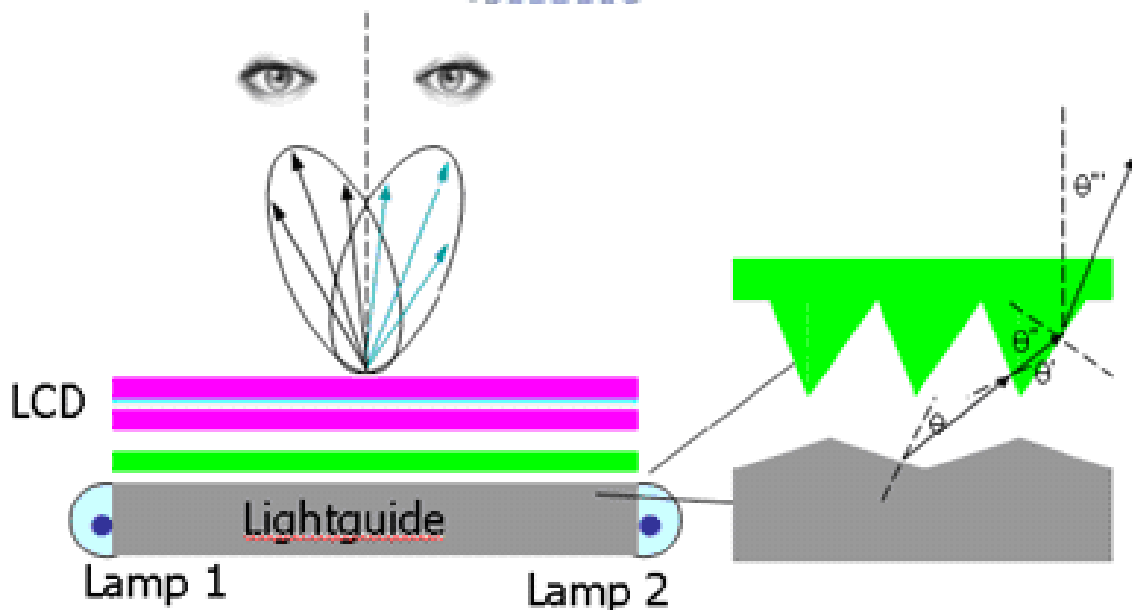
Fig. 1-8 3D display based on sequentially switching backlight with focusing foil.

As for the spatial-multiplexed type there also have many methods such as parallax barrier or lenticular array lens. Those are used to project the left and right image to different direction. And are currently the most mature 3D display technologies, and the basic principles of the resulting autostereoscopic displays are illustrated in the following section.

Parallax barrier

Parallax barrier [10],[11] is to use a simple series of opaque vertical lines to block the light from certain sub-pixel to viewer's left and right eyes as shown in Fig. 1-9. By optimizing the barrier geometry, adjusting the viewing window position and angles is possible. The main disadvantage is that the barrier reduces the brightness of the display.
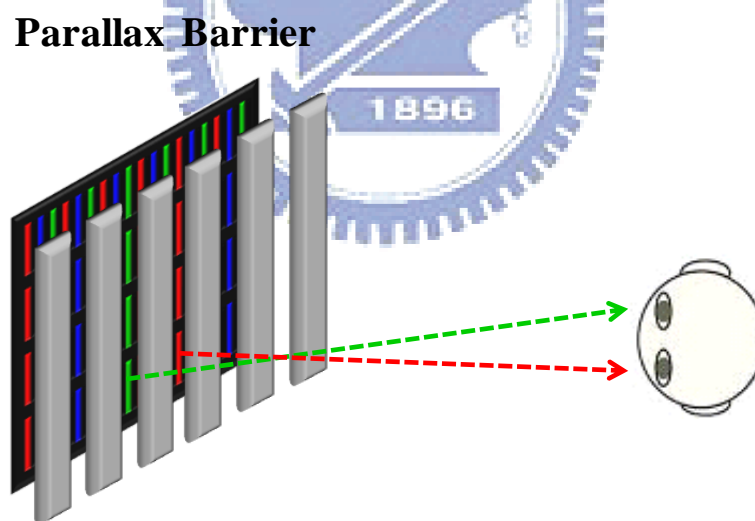
Fig. 1-9 Spatial multiplexed displays: parallax barrier.

Lenticular lens array

Lenticular lens [12],[13] use lenslets attached to the display with high accuracy. These lenses separate the image into left and right image as shown in Fig. 1-10. The main advantage of lenticular array lens is high brightness. But the disadvantage is reduction of resolution in one direction.

Lenticular lens array
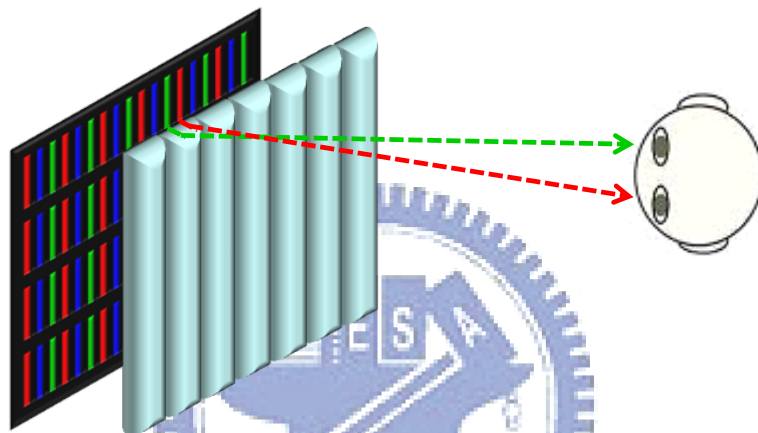
Fig. 1-10 Spatial multiplexed displays: lenticular array lens.

To overcome the problem of reduction of resolution in one direction, Philips proposed an approach using slanted lenticular lens [14],[15] to make the resolution loss is shared between horizontal and vertical (rather than unaffected vertical resolution and very low horizontal resolution) as shown in Fig. 1-11.

However, the issue of reduction of resolution still exists, Philips's design just makes the resolution become not too severe.
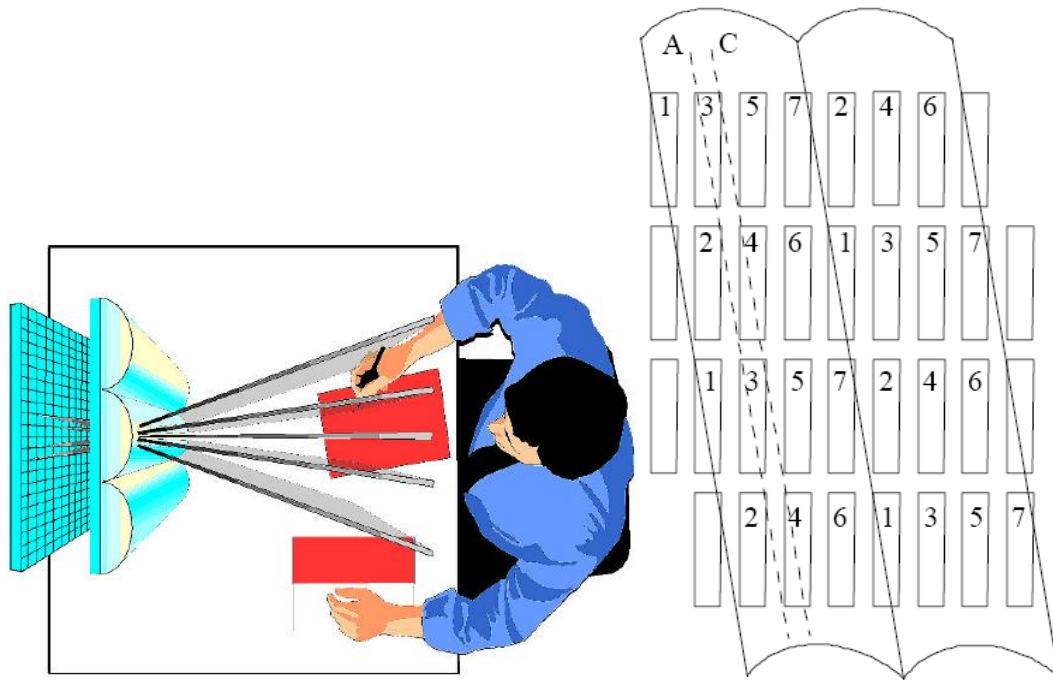
Fig. 1-11 Multi-view slanted lenticular lens by Philips.

1.3.4 2D/3D switching methods

The ability to switch between 2D and 3D images gives significant advantages to users who need both display type. Most users prefer to have the ability to switch between 2D and 3D modes, because they do not want to have two displays on their desk.

If a 3D autosteroscopic display is used to show 2D information, a distorted effect is often seen, particularly for text. This because each eye is still viewing a subset of pixels even if the data is no longer providing a stereo image pair. So, "turn off" the 3D function while viewing 2D image is desirable. There are a number of techniques that are able to perform this exchange. Current technology for 2D/3D switching includes active parallax barriers [16] and polarization activated micro lenses [17][19][20][21].

Active Parallax barrier

A series of barrier that is able to block the light, thus will give some freedom of switching between 2D and 3D as show in Fig. 1-12. When turning off the voltage the barrier has no function therefore can transmit the light completely. When turning on the voltage the whole device will act as a spatial-multiplexed parallax barrier type. However the light is absorbed by barrier patterns. Thus, the drawback of barrier is low brightness when displaying 3D images.
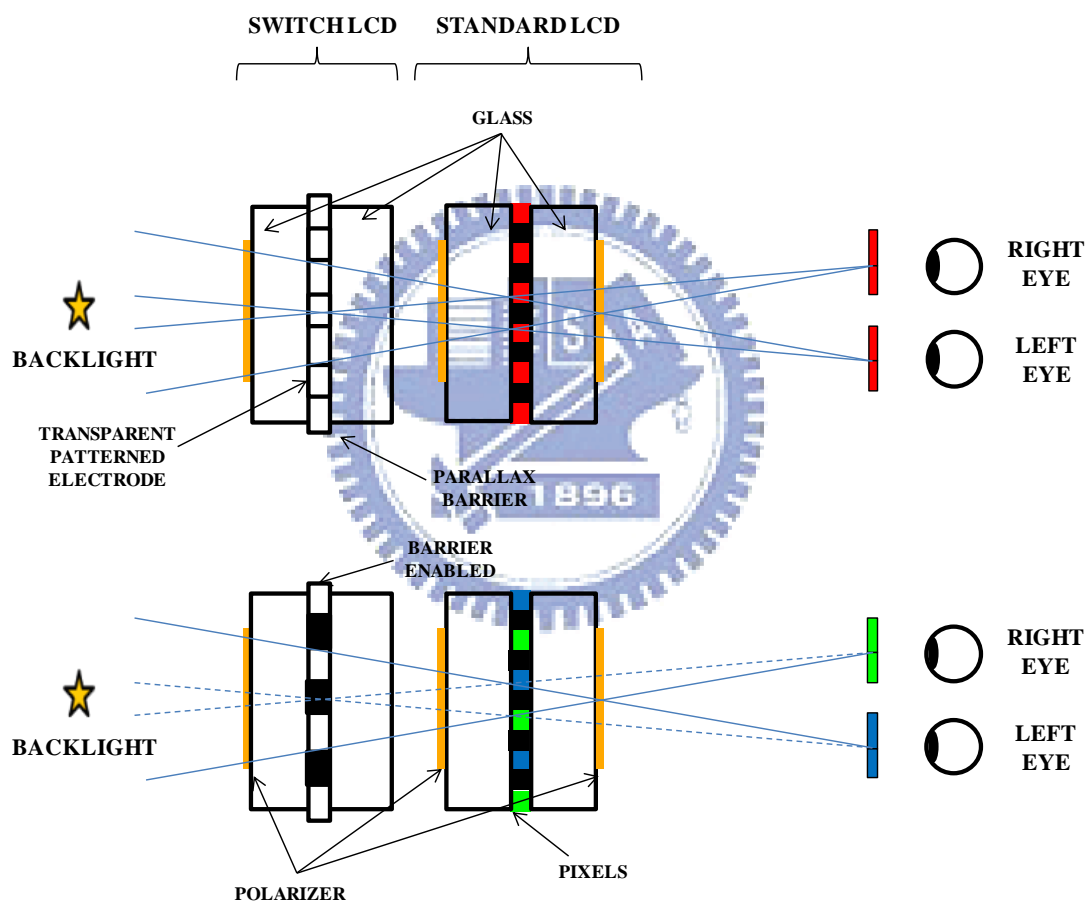
Fig. 1-12 2D/3D switching using Active Parallax Barrier.

Active Micro Lens

The use of an LCD equipped with lenticular lenses is a viable route to achieve multiview 3D displays. By using an active switchable LC lenticular lens, we can have a display that shows natural 3D images as well as high-resolution 2D [22]. Among various types of 3D displays, switching methods can be divided in to two categories such as the control of transmittance and the control of light direction, The former controls the transmittance of stripe barrier patterns using liquid crystal cell of parallax matrix. But because the light is absorbed by barrier patterns, its low brightness is a serious limitation in 3D modes.

On the other hand, for the latter case of controlling optical path, lens-switching methods are introduced such as polarization activated microlens [23], active LC lenticular lens [17],[18], and the electric-field driven LC lens (ELC lens) [19]. In the case of polarization activated microlens, anisotropic lens and polarization switching cell are used together to control the direction of polarized light as shown in Fig. 1-13 (a). In the case of active LC lenticular lens, concave lens patterns are formed inside switching LC cell and refractive index difference between LC and the geometrical concave shape controls the direction of incident light as shown in Fig. 1-13 (b). However, these designs are not compatible with current liquid crystal displays (LCDs) production infrastructure. Also, complete lesn-off state is difficult to achieve dues to a residual index mismatching around the interface between concave structure and liquid crystal molecules. In the case of ELC lens, the 2D/3D switching using the lens effect solely caused by LC director distribution under controlled non-uniform electric filed distribution.

(a)

(b)

(c)
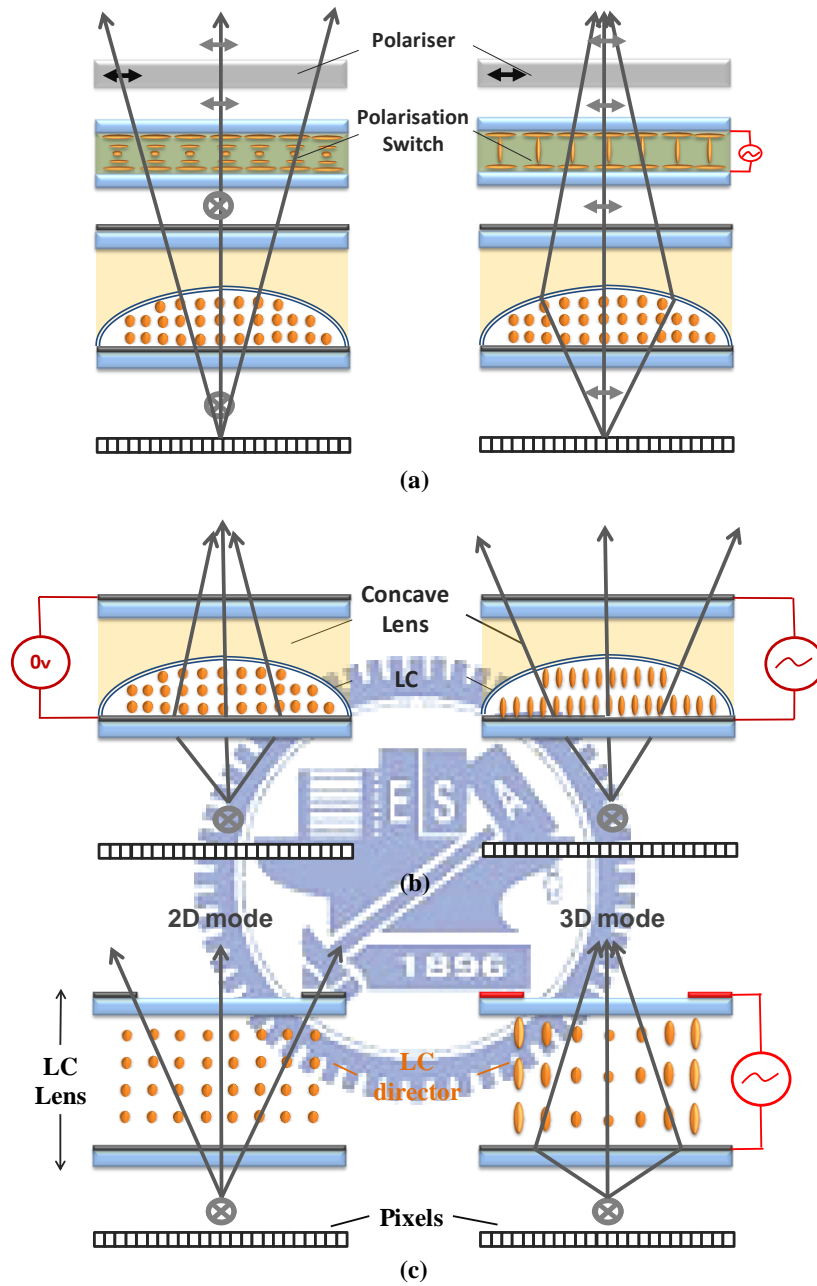
Fig. 1-13 Basic concepts of lens switching method reported previously. In case of (a), it is caused by the polarization switching of LC under anisotropic lens [23]. (b), the on/off switching is driven by the change of LC convex lens under the concave structure [17]. (c) the on/off switching is driven by electric field of electrode. [19]

1.4 Motivation and Objective

Display developments were driven by giving us more realistic image. Especially the 3D display has attracted the most interest. People want to see an image as natural as possible. However, 3D displays still encounter many issues that needed to be improved. The reduction of brightness of 3D display applying parallax barrier has less light efficiency than that of lenticular lens. However the lenticular lens 3D display still losses the resolution. The resolution loss depends on how many views the display can provide. Additionally, with using the lenticular lens is hard to switch between 2D and 3D images. Therefore, some methods of 2D/3D switching applying liquid crystal lens were proposed. However, they still faced with issues of mismatching of LC alignment at the interface of concave lens, as well as incompatible with current LC display production process. The first problem caused the image in project to the wrong direction and caused crosstalk.

In order to improve the mentioned issues, the **Multi-Electrically Driven Cylindrical Liquid Crystal (MeDLC)** Lens for 2D/3D switching display was proposed in this dissertation, utilizing non-uniform electric fields by multi-electrodes to yield 2D/3D switchable images. Compared with prior switching LC-Lens for 3D display, MeDLC lens are simpler and more competitive, which can avoid LC alignment issue. The phenomenon of crosstalk is less evident than that of conventional LC lens. Furthermore, the number of views can be increased by increasing the lens's pitch.

In this research thesis, we will focus on designing the MeDLC structure for the TV application, and to fit with the lens-like distribution. In this case, we can make sure our design can project the image to the right direction and therefore result in a smaller crosstalk phenomenon. Final is to achieve a workable switching.

1.5 Organization

This thesis is organized as following: The principle of liquid crystal, the focusing formula, and the principle of conventional 2D/3D switching method is presented in **Chapter 2**. Additionally, this chapter also shows the crosstalk phenomenon. In **Chapter 3**, the fabrication process of the MeDLC will be introduced in detail, and the major instruments used to measure the MeDLC images. The design and simulation result of MeDLC and discussion will be shown in **Chapter 4**. Next the experimental result and summary will be presented in **Chapter 5.** Finally, the conclusions and future work of this thesis will be given in **Chapter 6.**

Chapter 2

Principle of Liquid Crystal Lens

First, this chapter covers the principles of how the refractive index changes when liquid crystal faced different direction. Second, principle of lens and GRIN lens, and the focal length proof of a cylindrical lenticular lens will be discussed. Third, in order to design a 2D/3D switching display, the conventional double electrode LC lens and, the principles of conventional 2D/3D switching method are introduced. Finally, a brief summary will be given.

2.1 Introduction to liquid crystal

Liquid crystal can be divided into two groups: positive dielectric anisotropy and negative dielectric anisotropy. For positive dielectric anisotropy is that if the component along the optical axis is greater than the component perpendicular to the axis ($\varepsilon_{//} > \varepsilon_{\perp}$). These molecules align parallel to an applied field. If the reverse is true ($\varepsilon_{//} < \varepsilon_{\perp}$), than it is said to be negative dielectric anisotropy and the molecules will align perpendicular to an applied field. Either case can be apply for create a liquid crystal lens [24].

2.1.1 Liquid crystal orientation to match the index of refraction

Liquid crystals are characterized by an orientation order of their constituent rod like molecules. In nematic LC this orientation order has uniaxial symmetry, the axis of symmetry being parallel to a unit vector d called the director. Since the orientation of liquid crystal can be change when applying curtain voltage. This change will affect the direction of light when passing thru the liquid crystal layer because of the change of the refractive index in liquid crystal.

Refer to Fig. 2-1   assume light propagate in the z direction and polarized in x direction. When the indicatrix is not rotated the light will be affected by the refraction n_e. However when the indicatrix is rotated at an angle θ the same light will be affected by both n_e and n_o. The slice of the indicatrix can be expressed as Eq.2-1.
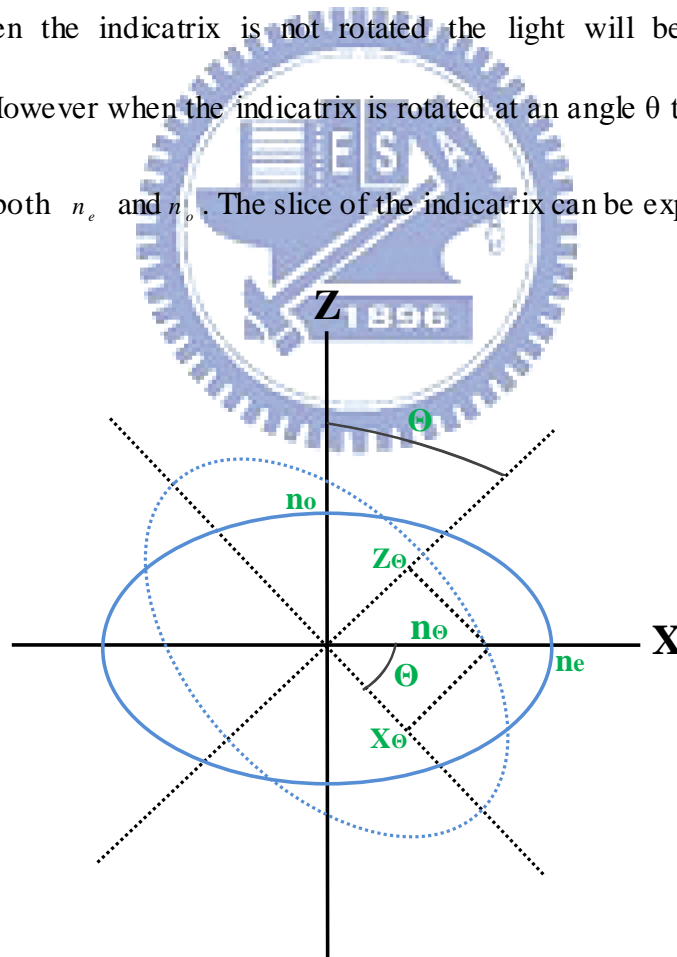
Fig. 2-1 Geometry to calculate change in index of refraction with liquid crystal

molecule orientation.

17

$$\frac{x_\theta^2}{n_e^2} + \frac{y_\theta^2}{n_o^2} = 1 \qquad (2\text{-}1)$$

And

$$n_\theta^2 \approx x_\theta^2 + y_\theta^2 \qquad (2\text{-}2)$$

Therefore, Eq.2-1 can be written as Eq.2-3.

$$\frac{n_\theta^2 - y_\theta^2}{n_e^2} + \frac{y_\theta^2}{n_o^2} = 1 \qquad (2\text{-}3)$$

Equivalently,

$$y_o = \sqrt{\frac{(1 - \frac{n_\theta^2}{n_e^2})}{(\frac{1}{n_o^2} - \frac{1}{n_e^2})}} \qquad (2\text{-}4)$$

Thus the equivalence equation of rotate angle can be derived as Eq.2-5.

$$\theta = \sin^{-1} \sqrt{\frac{(\frac{1}{n_\theta^2} - \frac{1}{n_e^2})}{(\frac{1}{n_o^2} - \frac{1}{n_e^2})}} \qquad (2\text{-}5)$$

Since the nematic liquid crystal does not align uniformly across the cell in the thickness direction, a more useful form can be obtained to solve the n_θ as Eq.2-6.

$$n_\theta = \frac{n_e}{\sqrt{1 + \sin^2 \theta [(\frac{n_e^2}{n_o^2} - 1)]}} \qquad (2\text{-}6)$$

This expression gives the index of refraction for light polarized in the x direction and traveling in the z direction as a function of the angular orientation of the nematic liquid crystals in the x-z plane. Therefore, can be applied when the LC direction were no longer perpendicular or parallel to the x direction.

2.2 Introduction to Gradient Index Optics

A conventional lens explains how Gradient Index Lens (GRIN lens) is works: An incoming light ray is first refracted when entering the shaped lens surface this is caused by an abrupt change in the refractive index from air to the homogeneous material. The light passes the lens material in a direct way until it emerges through the exit surface of the lens where it is refracted again because of an abrupt index change from the lens material to air, as shown in Fig. 2-2.
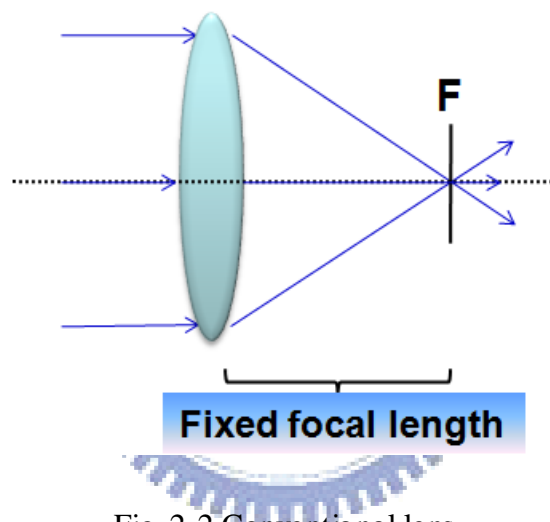
Fig. 2-2 Conventional lens

GRIN is short for graded-index or gradient index which can refers to an optical element in which the refractive index varies. More specifically (from the Photonics Dictionary) a GRIN lens is a lens whose material refractive index varies continuously as a function of spatial coordinates in the medium. Also, a graded-index fiber describes an optical fiber having a core refractive index that decreases almost parabolically and radially outward toward the cladding as shown in Fig. 2-3. However the focal length of GRIN is fixed [26][27].
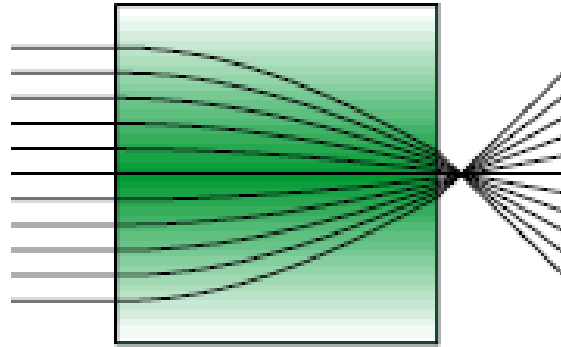
Fig. 2-3 GRIN Lens

Fig. 2-4, shows the geometry of the focused GRIN lens. First we assume $f > r$ and a center refractive index value of the center larger than the edge. And as the known formula, $v = c/n$, where c, n and v are the velocity in vacuum, index of refraction and the velocity in medium. Using $v = c/n$ we know the velocity is inverse proportional to the refractive index. Therefore, wave fronts will slow down when reaching the dense region and speed up in less dense regions. In this case the GRIN lens can be focused.
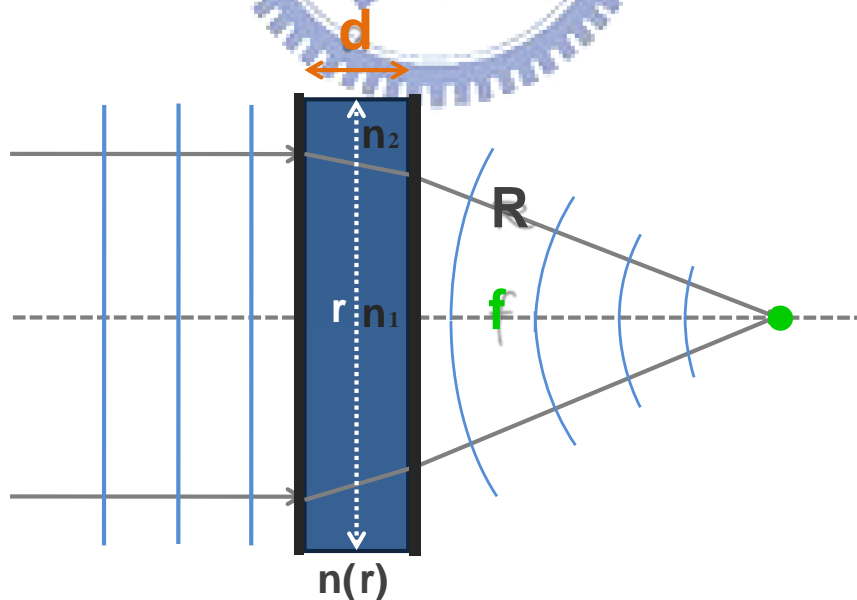
Fig. 2-4 The geometry of the focused GRIN Lens.

A ray that traverses the lens on the optical axis passes along an optical path length (OPL) of $(OPL)_{axis} = n(r')_{max}d$,whereas for a ray traversing at a height $r' = \dfrac{r}{2}$, overlooking the slight bending of ray path, $(OPL)_r \approx n(r')d$. Since a planer wave front must be bend into a spherical wave fronts, the OPLs from one to the other, along any route must be equal as followed,

$$R^2 = (r')^2 + f^2 \tag{2-7}$$

and

$$n_1d + f = n_2d + R \tag{2-8}$$

By substitution of Eq.2-7 and Eq.2-8 can get,

$$f = \frac{r^2 - [(n_1 - n_2)d]^2}{2(n_1 - n_2)d} \tag{2-9}$$

Where $n_1 - n_2$ in the refractive index difference between center and the edge (Δn), if Δnd can be neglect, at last we can get the focusing formula as Eq.2-10.

$$f = \frac{r^2}{2(\Delta n)d} \tag{2-10}$$

By substitution, we can get,

$$\Delta n = \frac{r^2}{2 \cdot d \cdot f} \tag{2-11}$$

where Δn can equal as a parabolic function with a constant α.

$$\Delta n = \alpha \cdot r^2 \tag{2-12}$$

As the result, if the index of refraction drops off parabolically from its high along the central axis, the GRIN lens would focus at point F. However, GRIN lens can only be operated as a lens with fixed focal length. Hence, the application of LC lens became more useful. The LC lens can be acted as both GRIN lens with variable focal length and normal layer with certain refractive index by controlling the direction of LC direction. In this case, the ability of switching between 2D and 3D images can be achieved, which will be demonstrated detailly in next section.

2.3 Conventional LC lens

For a conventional liquid crystal lens [28] where the focal length is defined in Eq. 2-10. The LC direction can be controlled by the applied voltages between two parallel electrodes, owning to the fringing field effect as shown in Fig. 2-5. Passing through this lens, light encounters different refractive indexes so that the changes of phase retardation work as a lens, and refracts light to different angle. However, when applying a low operation voltage the electric field cannot affect the liquid crystal near the center efficiently and its equivalence lens results in a small numerical aperture (large focal length) as shown in Fig. 2-6 (a). So that the lens has to place in a long distance and cause a large volume of display which is not suitable for the market place. Although a high operation voltage can cause a higher numerical aperture. However due to this high voltage the LC directory near the edge of the LC cell will show no distinct difference. Therefore, the equivalence lens can result in a multi focal length lens as shown in Fig. 2-6 (b). Which will result in a large beam size and therefore cause a high crosstalk phenomenon as shown in Fig. 2-7 (a) and Fig. 2-8 (a). For a comparison, an ideal lens which with smaller bean size will result in a small crosstalk

phenomenon as shown in Fig. 2-7 (b) and Fig. 2-8 (b).

This method not only solves the issue of mismatching of LC alignment, but also LC lens production incompatibility. Nevertheless, this method has a drawback of high operation voltage large beam size and result in high crosstalk.
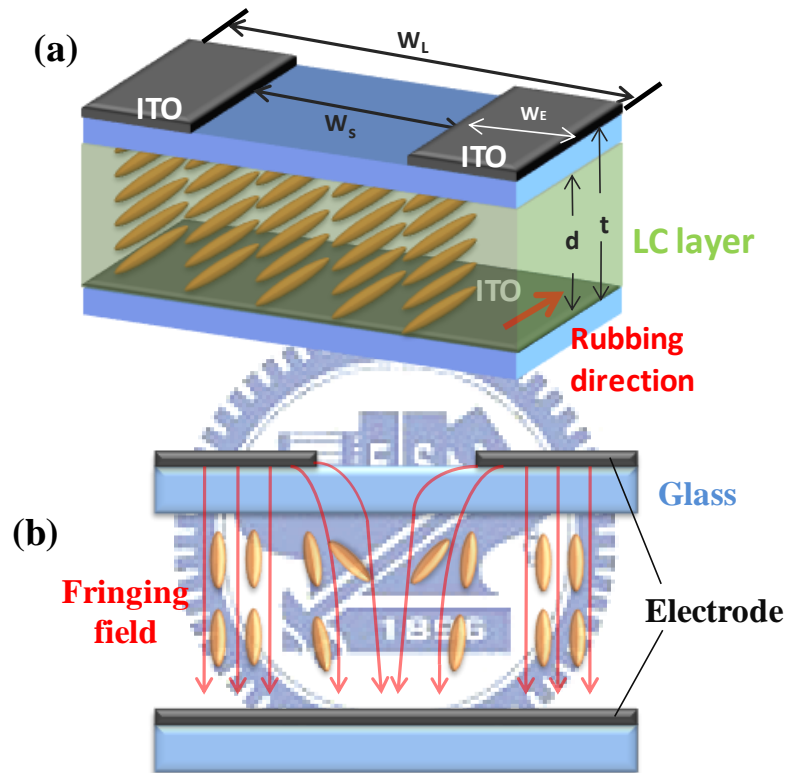
Fig. 2-5 Structure of the traditional LC cylindrical lens

(a) Top view and (b) Side view.
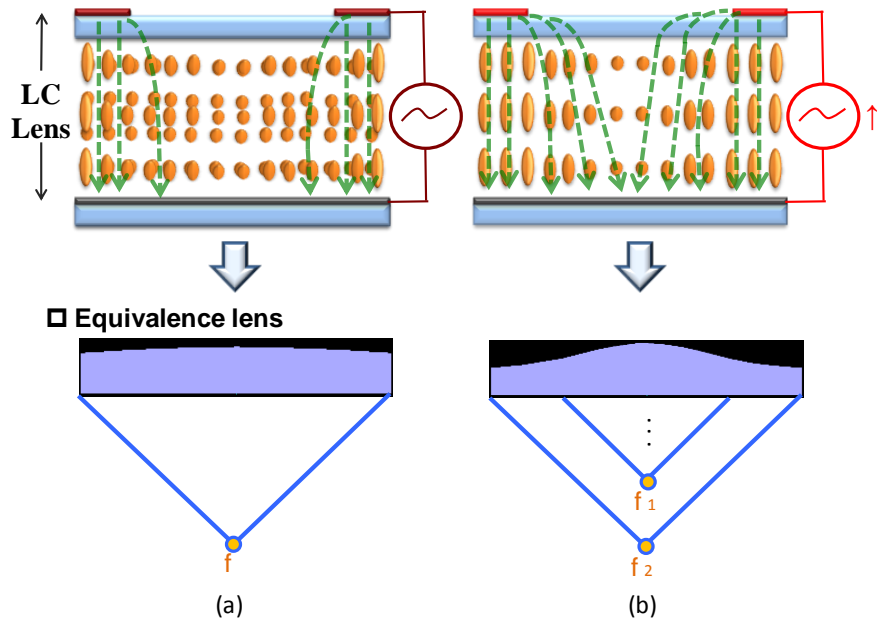
Fig. 2-6 The fringing field effect of a double electrode lens

(a) an equivalence lens when applying low operation voltage

(b) an equivalence lens when applying high operation voltage
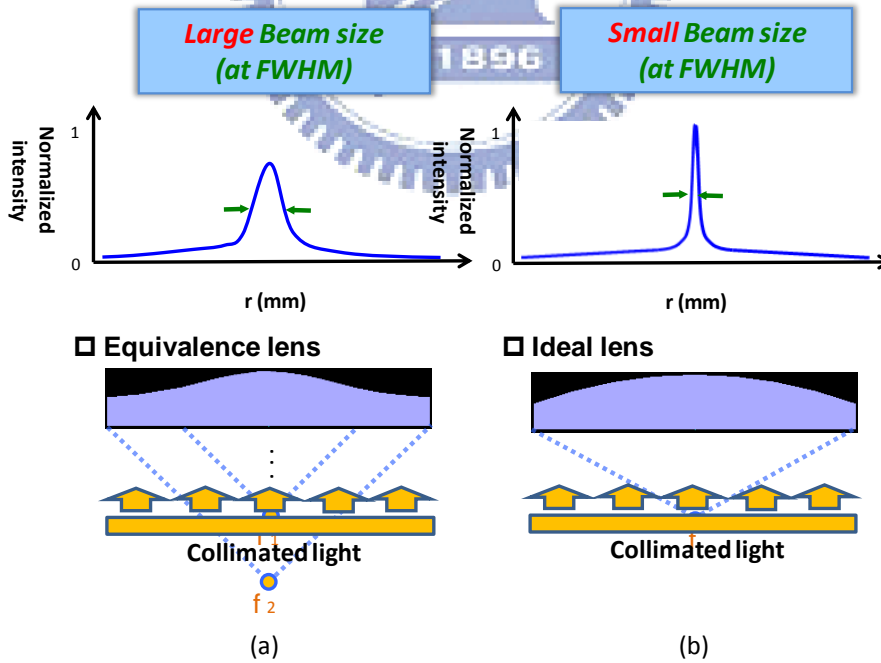
Fig. 2-7 The beam size of (a) equivalence lens of double electrode LC lens when

applying large operation voltage (b) ideal lens
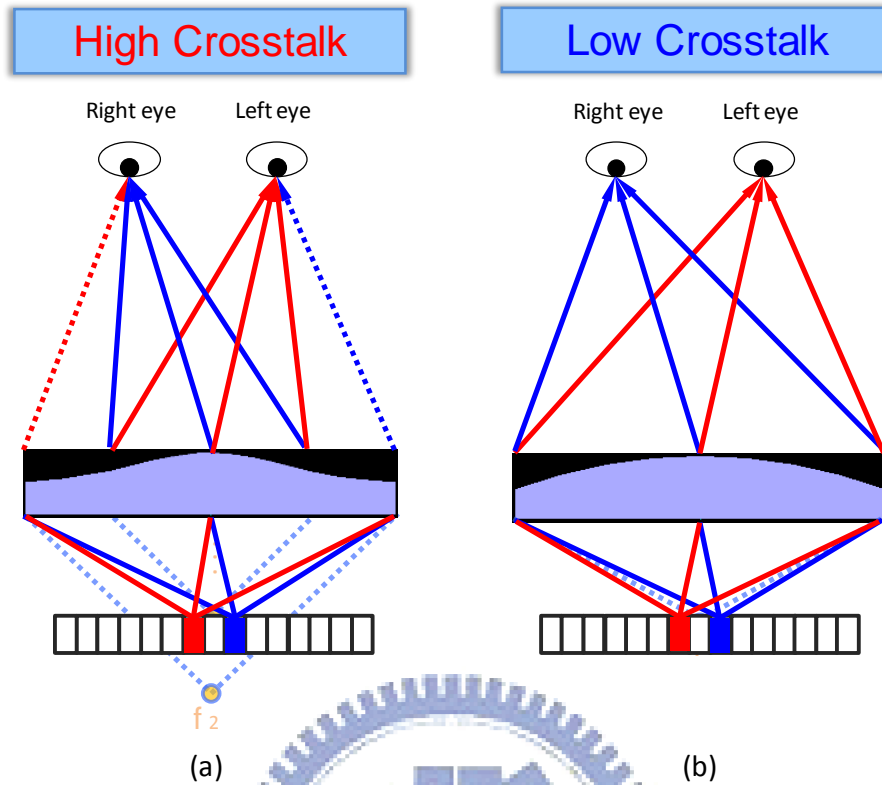
Fig. 2-8 The crosstalk of (a) equivalence lens of double electrode LC lens when

applying large operation voltage (b) ideal lens

2.4 LC lens with 2D/3D switching

Among various types of 3D displays, switching methods can be divided into two

categories such as the controls of transmittance and the control of light direction. For

the latter case of controlling optical path, lens switching methods are introduced such

as active LC lenticular lens and polarization activated microlens.

2.4.1 Active LC Lenticular lens

In the case of active LC lenticular lens as shown in Fig. 2-9. A fixed concave lens patterns were formed inside the cell and the LC were placed between the concave lens and bottom substrate, which only the refractive index of n_o is the same as the concave lens. If the light from the underlying LCD display is polarized perpendicular to the plane of the drawing, it encounters a refractive index transition from high to low within the cell, resulting in a net lens-action to form a 3D image.

If a voltage is applied over the cell, the extra-ordinary axis of the LC is aligned parallel to the lens axis, which is in the plane of the drawing. Therefore, the light encounters the lower refractive index corresponding to the ordinary axis of the LC. Since the ordinary refractive index matches the refractive index of the concave lens, the lens is effectively switched off. In this case 2D images can be perceived.
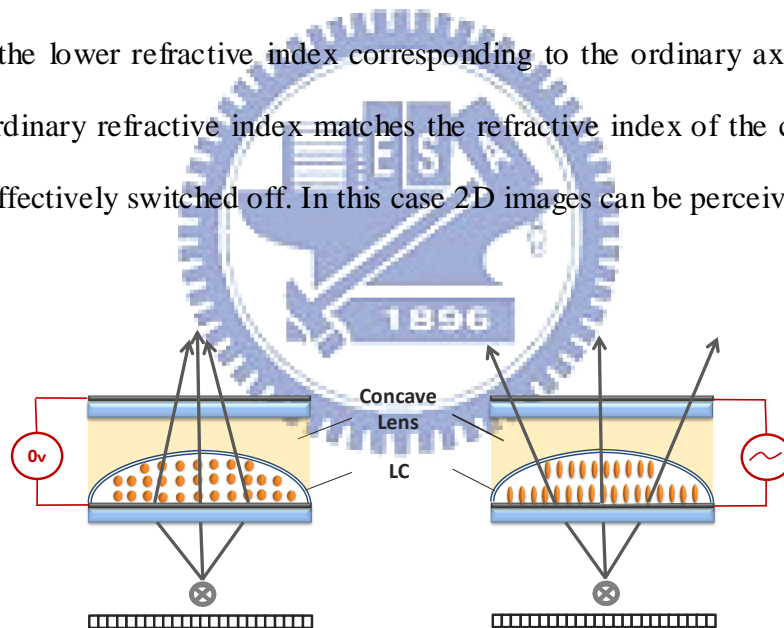
Fig. 2-9 Principle of active LC lenticular lens

2.4.2 Polarization activated microlens

For the polarization activated microlens as shown in Fig. 2-10. The light was polarized, and the light direction was changed after encounter with different refractive in the micro lens. The ability of switching between 2D and 3D images can be achieved by applying voltage to the polarization switch layer.
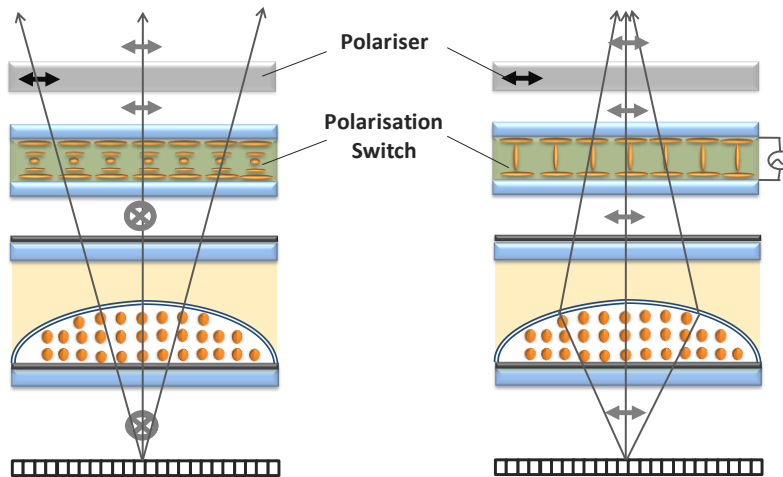
Fig. 2-10 Principle of polarization switch LC lens

However these two methods have some disadvantages, such as mismatching of LC alignment at the interface of concave lens, as well as incompatible with current LC displays production process and brightness.
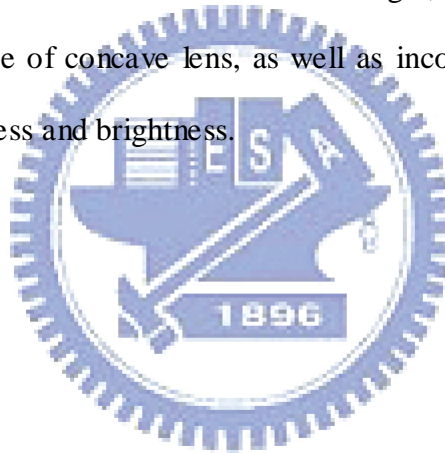
2.4.3 Electric-field driven LC lens (ELC lens)

Fig. 2-11 shows the basic concept of electric-field driven LC lens for one lens pitch. At the voltage off state, incident light passes through ELC lens cell without change of propagation direction. At the voltage on state, local electric fields are formed. The electric field at the part of lens edge is much stronger than electric field at center of lens. This non uniform distribution of electric field cause non uniform of tilt angle of LC director and the refractive index changes accordingly. Therefore, a phase difference was achieved and cause the change of propagation direction of the light. In this case, a 3D image can be perceived.
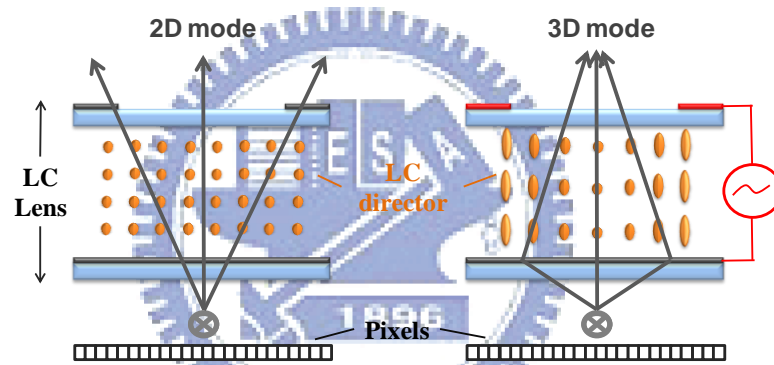
Fig. 2-11 Concept of electric-field driven LC lens at (a) lens off state for a 2D mode

(b) lens on state for a 3D mode.

For a short summary the conventional double electrode LC lens have the drawback high operation voltage, large beam size and result in a high crosstalk of 3D display. And the methods of Active LC Lenticular Lens and Polarization activated microlens have the issue of mismatching of LC alignment and incompatible of LCD current production.

2.5 Crosstalk phenomenon of LC-lens on 3D displays.

In our opinion the use of an LCD equipped with lenticular lenses is a viable route to achieve multi-view 3D display. By using a switchable LC lenticular lens, we can have a display that shows natural 3D images as well as high-resolution 2D material. And thus the most dominating characteristic affecting on the perceived stereo image quality in 3D displays is the 3D crosstalk. The crosstalk affects not only to how easily the image can be fused and how smooth the transition between adjacent views is, but also to the overall image quality, being in the worst case a source of visual discomfort. 3D crosstalk can be defined as the leakage of the left eye image data to the right eye. This also indicating the images for each eyes must be well project. As for the application of using lens to provide 3D as shown in Fig. 2-12. The crosstalk phenomenon can be minimized when the image can be projected to the exact eyes, under the condition of the having high focusing ability of the lens. If a LC lens with low focusing ability than the left-eye image data will leak to the right–eye and vice versa, therefore these wrong image signal can cause high crosstalk phenomenon. And the crosstalk value definition is as shown in Eq.2-13 [19].
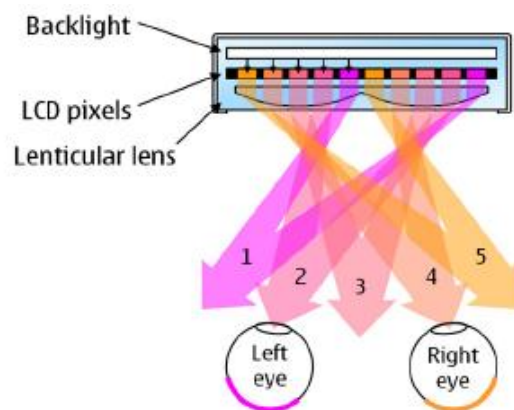
Fig. 2-12 Examples of 3D displays working principle of lenticular lens.

29

$$\chi = \frac{I_{\min}}{I_{\max} + I_{\min}} \times 100 \; [\; \% \;] \qquad\qquad (2\text{-}13)$$

2.6 Summary

Some important principle of liquid crystal and the conventional LC lens have been discussed briefly in this chapter. We present the fundamental theory of refractive index difference when liquid crystal was no longer parallel or perpendicular to the light direction. This can give us the idea of how to let the incoming light to project to different direction. Followed by the basic focusing principle of a cylindrical lens can show the formula of focal length. Third the conventional LC lens was discussed. These give us the idea of how to operate the liquid crystal lens. Finally, the definition of crosstalk for 3D images was illustrated.

From prior reports, active LC-lens plays an important role in 3D-display technology not only it can be used in 2D/3D images switching but also can be combined with a head tracking device. In this case a high resolution and wide viewing angle 3D images can be perceived.

In this thesis, these fundamental work principles are employed for designing the new LC lens for enhance the mismatching of LC alignment, production process, effective aperture, and the crosstalk phenomenon.

Chapter 3

Fabrication and measurement Instruments

3.1 Introduction

The process to fabricate LC lens were described in this chapter. The commercial available indium-tin oxide (ITO) glass which thickness is 550 μm and the resistance is 20Ω/□ was cleaned by standard process in advance. After that, the semiconductor process including spin coating, lithography and etching was utilized in order to obtain the desired pattern. Followed by the spin coating and rubbing techniques to make the alignment layer. Next, the top and bottom glass was assembled which the cell gap was controlled about 60 μm by spacers and fill in the LC. Finally, wires for various voltage driving will be connected to each electrode.
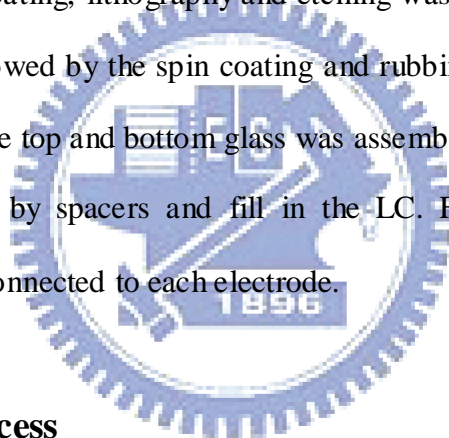
3.2 Fabrication process

This part will describe the cell fabrication process which includes spin coating, lithography, wet etching, rubbing, assembling. The detailed fabrication steps are listed below and as shown in Fig. 3-1. Also the ITO patterning is shown schematically in Fig. 3-4.

```
                    ┌─────────────────────┐
                    │   Glass Cleaning    │
                    └─────────────────────┘
         ┌───────────────────────┴───────────────────────┐
┌─────────────────────┐                         ┌─────────────────────┐
│    Shadow Mask      │                         │   Etching Solution   │
│    Preparation      │                         │     Preparation      │
└─────────────────────┘                         └─────────────────────┘
         └───────────────────────┐
                    ┌─────────────────────┐
                    │    Lithography      │
                    └─────────────────────┘
                    ┌─────────────────────┐
                    │      Etching        │
                    └─────────────────────┘
                    ┌─────────────────────┐
                    │    OM Checking      │
                    └─────────────────────┘
                    ┌─────────────────────┐
                    │     Patterned       │
                    │   Glass Cleaning    │
                    └─────────────────────┘
                    ┌─────────────────────┐
                    │      Coating        │
                    └─────────────────────┘
                    ┌─────────────────────┐
                    │      Rubbing        │
                    └─────────────────────┘
                    ┌─────────────────────┐
                    │     Assembling      │
                    └─────────────────────┘
                    ┌─────────────────────┐
                    │     Soldering       │
                    └─────────────────────┘
```
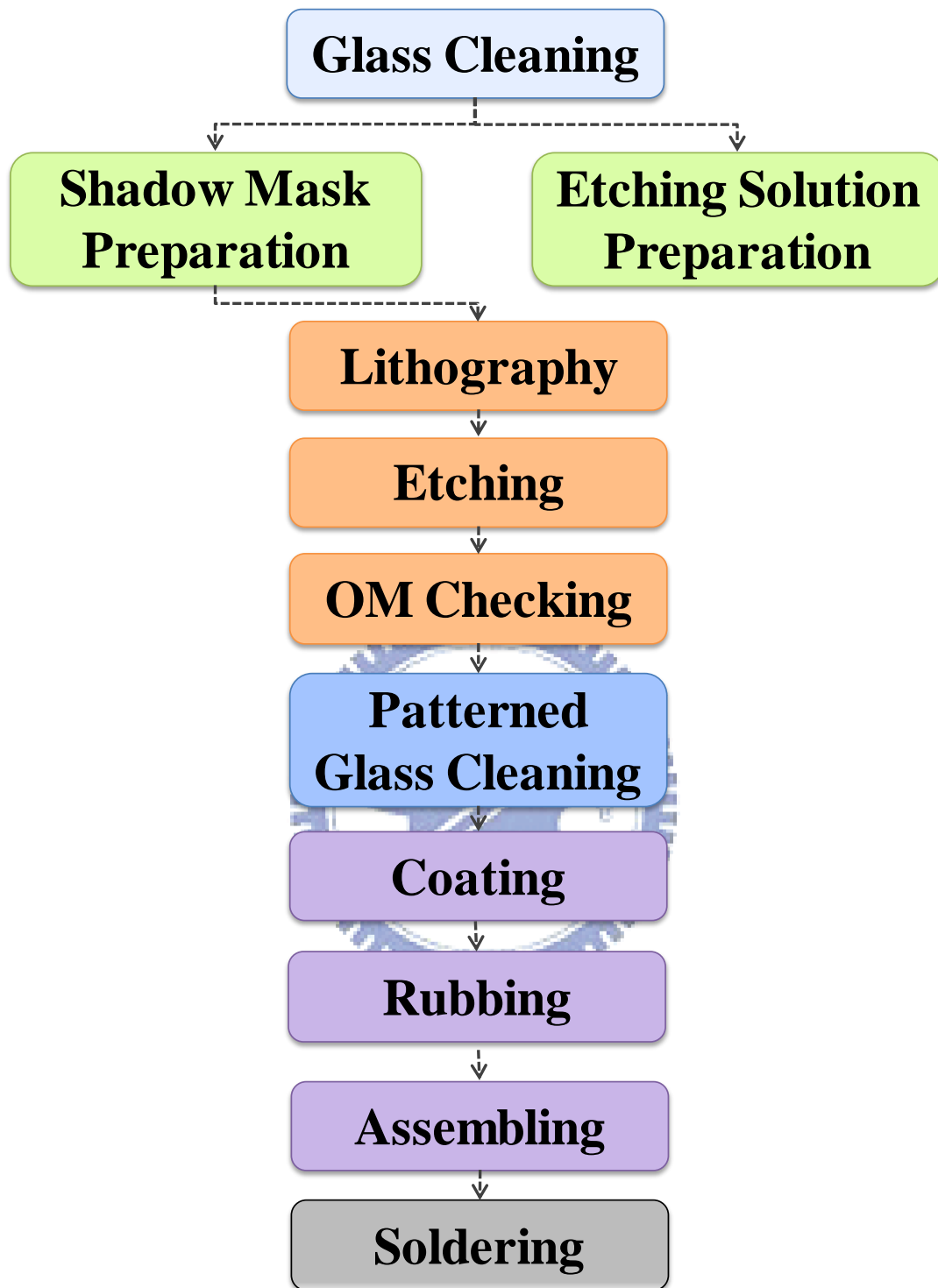
Fig. 3-1 Fabrication steps.

I. Glass cleaning

The detailed sequence is as follow:

Step 1: Place the glasses on the Teflon carrier, and put them into a container with acetone as shown in Fig. 3-2. Ultrasonic vibrates 20 minutes to remove the organic contamination on the glass.

Step 2: Rinsed by DI water 1 minute.

Step 3: Rubbing the glass with hand by detergent.

Step 4: Place the glasses on the Teflon carrier, and put them into a container with DI water as shown in Fig. 3-2. Ultrasonic vibrates 40 minutes to remove the remained particle and detergent on the glass.

Step 5: Use N_2 purge to dry the ITO glasses; Place them into a glass container with a cover.

Step 6: Put the glass container into an oven with $110^\circ C$ for 30 minutes.

Fig. 3-2 Schematic picture of step1 and step 4.

II. ITO patterning

The detailed sequence is as follow and also can refer to Fig. 3-4.
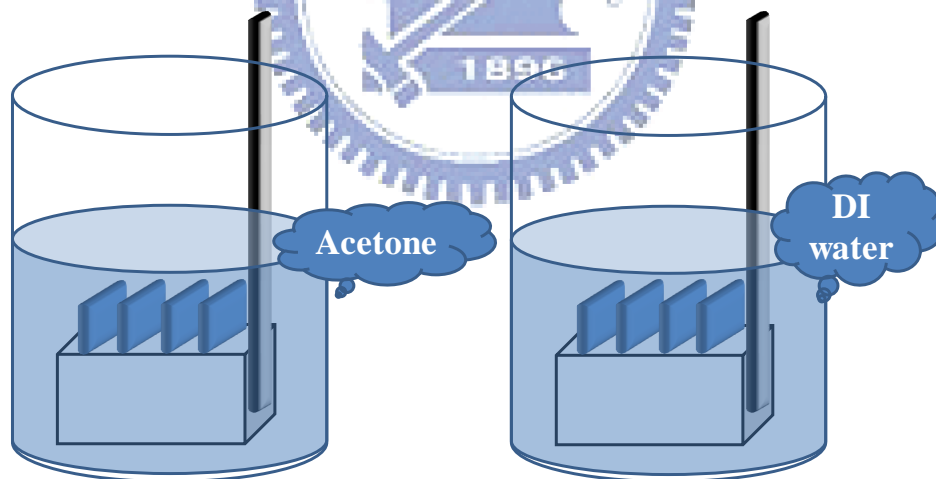
Step 1: For the display application, the glass is widely used as a substrate. In the fabrication, the ITO glass of about 0.55 mm thick was chosen. Before the lithography process, ITO glass was cleaned by step I.

Step 2: Put the glasses on the metal holder and put into the HMDS oven. The purpose is to eliminate the surplus steam and HMDS can improve the adhesion between organic photoresist and the glass, to let the phototresist can be uniformly coating on the substrate.

Step 3: A positive photoresist was applied and coated on substrate.

Step 4: Soft bake for one and a half minutes, to eliminate most of the solvent of the photoresist, to enhance the adhesion.

Step 5: Expose the ITO glass with ultra-violet (UV) light source through shadow mask for 40 second. Consequently, the pattern on the mask was transformed to the positive photoresist after developing. The MASK is as shown in Fig. 3-3.

Step 6: After exposure and development, the substrate was etched. And check by OM to see if there is any broken line.

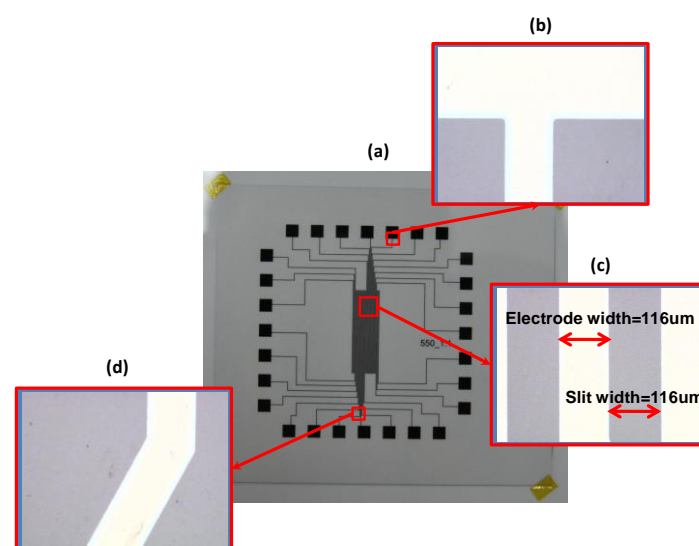Step 7: Remove the photoresist by acetone.

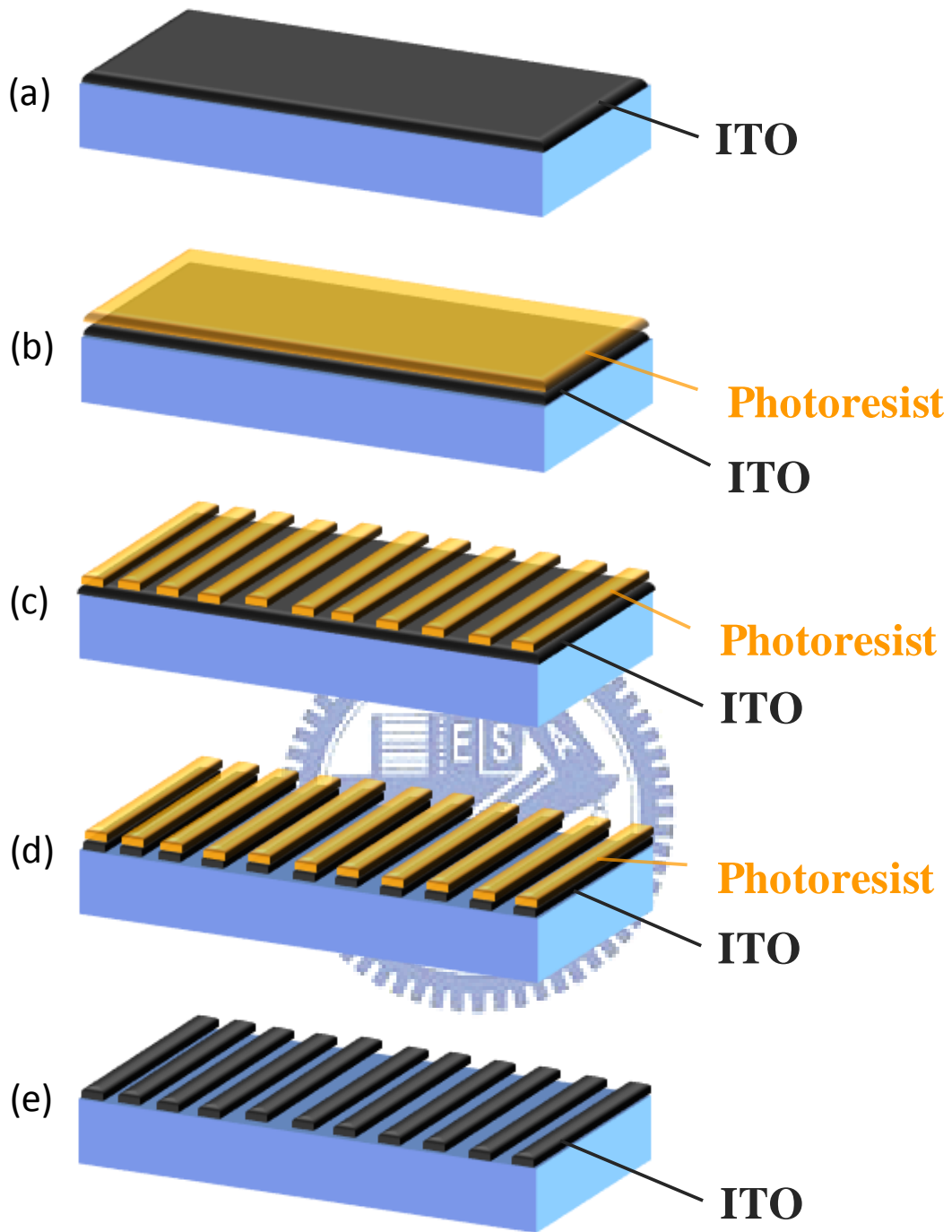Fig. 3-3 (a)The MASK pattern (b)(c)(d) is the pattern after etching.

Fig. 3-4 Flow of fabricating ITO electrodes.

(a) ITO glass,

(b) spin-coating Positive photoresist upon the ITO surface,

(c) using lithography technique to obtain the latent image,

(d) etching to produce the desired ITO pattern, and

(e) eliminating the remaining photomask by acetone.

III. Coating , Rubbing & Assembling

Step 1: Cleaning the patterned and bottom glass with the steps discussed previous.

Step 2: Put the glasses into the O-zone machine for 20 minutes, to eliminate the organic on the glasses, this step can make the coating more efficiently.

Step 3: Coating the solvent to make the PI adhesion more efficiently.

Step 4: Coating the PI.

Step 5: Put the glass container into an oven with 220℃ for 60 minutes.

Step 6: Rubbing the glasses and make the mark of the rubbing direction.

Step 7: Stick the plastic spacer on the bottom glass.

Step 8: Put the bottom glass on the top of the patterned glass and fixed with a tape.

Step 9: Put a heavy metal on the top of the glasses and glued.

Step 10: Fill in the LC

Step 11: Seal with non-bubbles glue and curing.

Next, the ultrasonic solder was soldered on the electrode to enhance the adhesive of the solder and smeared with AB glue to avoid the wires coming off. Finally, the Multi-Electrically Driven Cylindrical Liquid Crystal (MeDLC) will be measured.
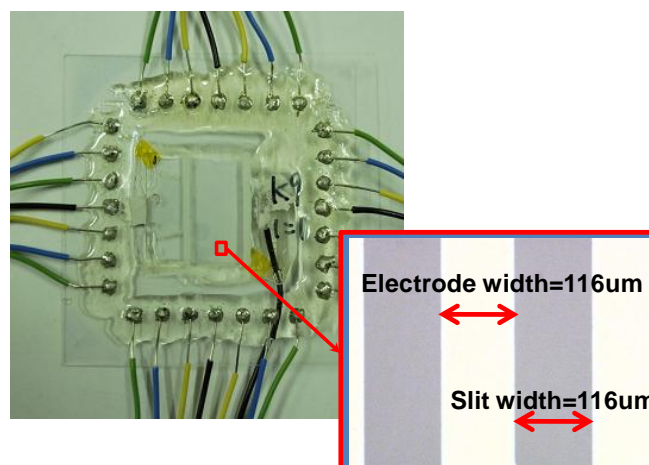
Fig. 3-5 Prototype of MeDLC

3.3 Measurement system

After the fabrication of MeDLC structure. The optical properties of the devices were measured by CCD; the setup is as shown in Fig. 3-6 and Fig. 3-7. First, the bright and dark lines can be recorded by the camera with cross polarizer. These lines were caused by the phase difference, and the profile of refractive index difference can be reconstructed, than the ideal curve and simulation result can be compared to check for the trend and performance of the MeDLC.

Fig. 3-6 Experiment setup

Fig. 3-7 Experiment setup

The method of tuning the voltage to an optimized value was shown as Fig. 3-8. First we transfer the Δn profile into x axis only as show in Fig. 3-8(b). Each dot represents a phase difference in 2π which als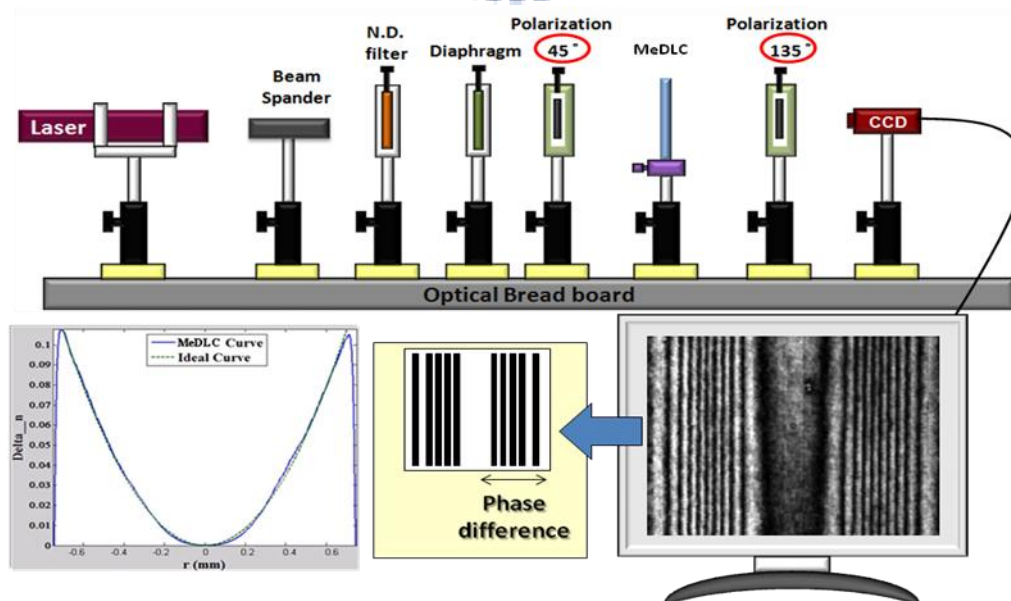o means the position when two bright or dark lines occur. Final is tried to find an optimized value of voltage that consist with these lines. Eventually, we can get an optimized value of operation voltage and a lens-like distribution.
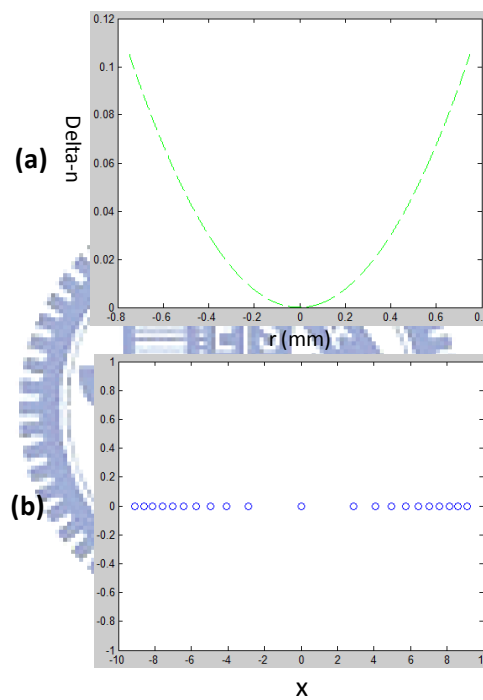
Fig. 3-8 (a) Ideal curve (b) equivalent position of Δn in the x direction

Finally, the beam size can be checked by setting the polarizer to be parallel to the electrode direction of MeDLC, as shown in Fig. 3-9. The LC direction can be controlled by the voltage. Thus the MeDLC will be able to act as a GRIN lens and be focused at certain point. Through this way the focal length and beam size can be found.

In our experiment, the MeDLC were measured by these two methods. And the results will be given in chapter5.

Fig. 3-9 Experiment setup

Chapter 4

Design of Multi-Electrically Driven Cylindrical Liquid Crystal Lens (MeDLC)

This chapter covers the MeDLC structure design and simulation result. First, the issues of conventional 2D/3D switching and conventional LC lens using double electrode were discussed. Second, a detail ideal of lens switching wil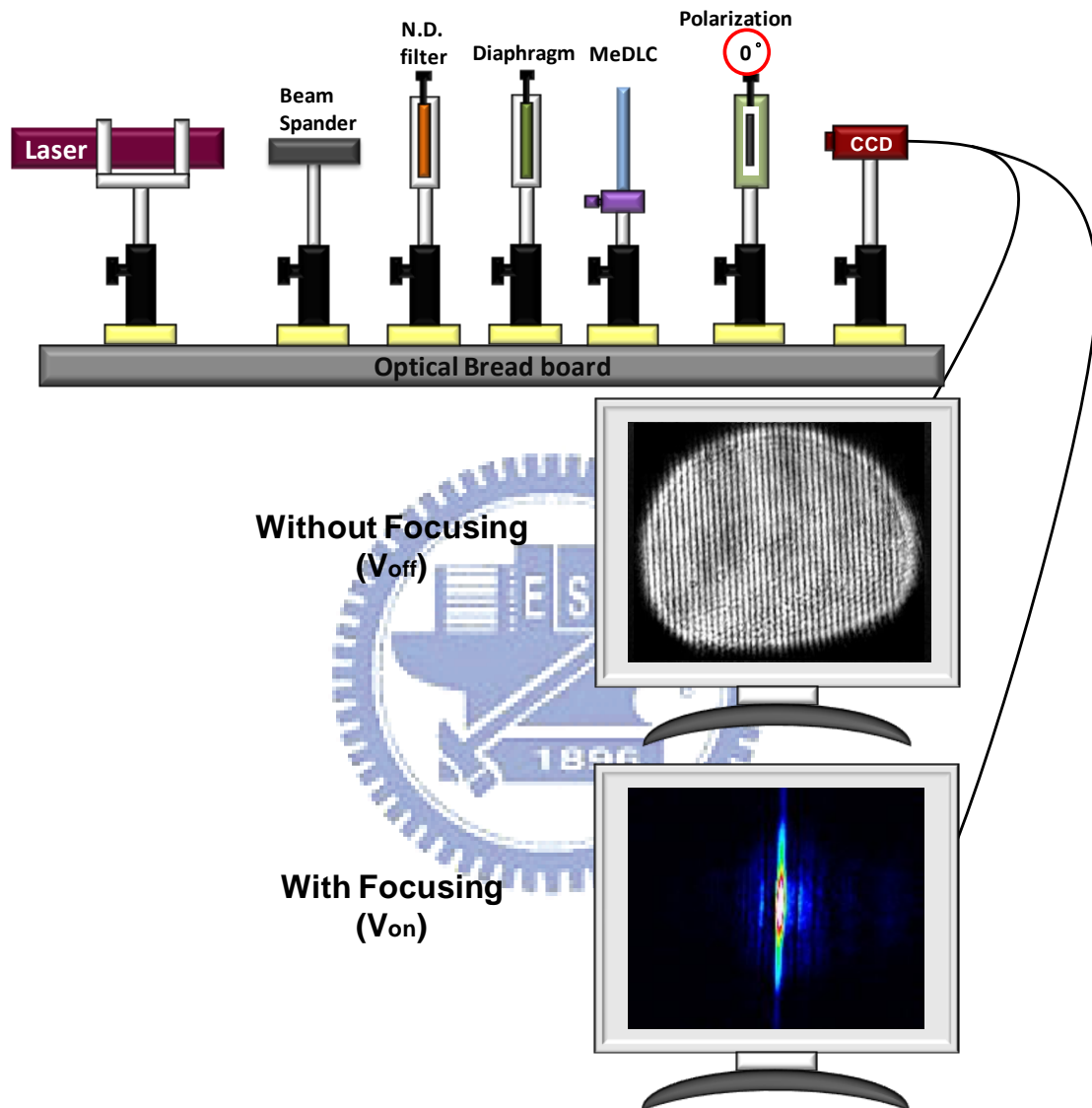l be explained. Third, the concept of our simulation steps and simulation result will be illustrated. Finally, a brief summary will be given.

4.1 Issues of conventional 2D/3D switching technologies

As mentioned in Chapter 1, among various types of 3D displays, switching methods can be divided into two categories such as the control of transmittance and the control of light direction. The former controls the transmittance of stripe barrier patterns using liquid crystal cell of parallax matrix. However, due to the light is absorbed by barrier patterns, its low brightness is a serious limitation in 3D modes. For the latter case of controlling optical path, lens switching methods were introduced such as actively switched lens and polarization active lens. However, these two methods suffer the issues of mismatching of LC alignment and LC lens production incompatibility.

Moreover, another method of controlling optical path is using double electrodes to form a lens function. However, the convention double electrode LC lens suffers the issues of high operation voltage and large beam size, hence cause serious crosstalk phenomenon. Therefore, we proposed a novel method using MeDLC to overcome this issue.

4.2 Introduction to MeDLC

A basic concept of Multi-Electrically Driven Cylindrical Liquid Crystal Lens (MeDLC) was shown in Fig. 4-1. At the voltage off state, incident light passes through MeDLC lens cell without change of propagation direction. At the voltage on state, local electric fields were formed. The electric field at the part of lens edge is much stronger than electric field at center of lens. This non uniform distribution of electric field causes refractive index changes accordingly. Hence, a non uniform distributions of tilt angle of LC director was formed. For the incident light having linear polarization with respect to the rubbing direction of MeDLC lens cell. The wave front were affected by differently distributed refractive index, thus the propagation direction were changed. By making repeated patterns, lenticular LC lens array structure can be obtained. Eventually, the images can be refract to different angle to form 3D images.
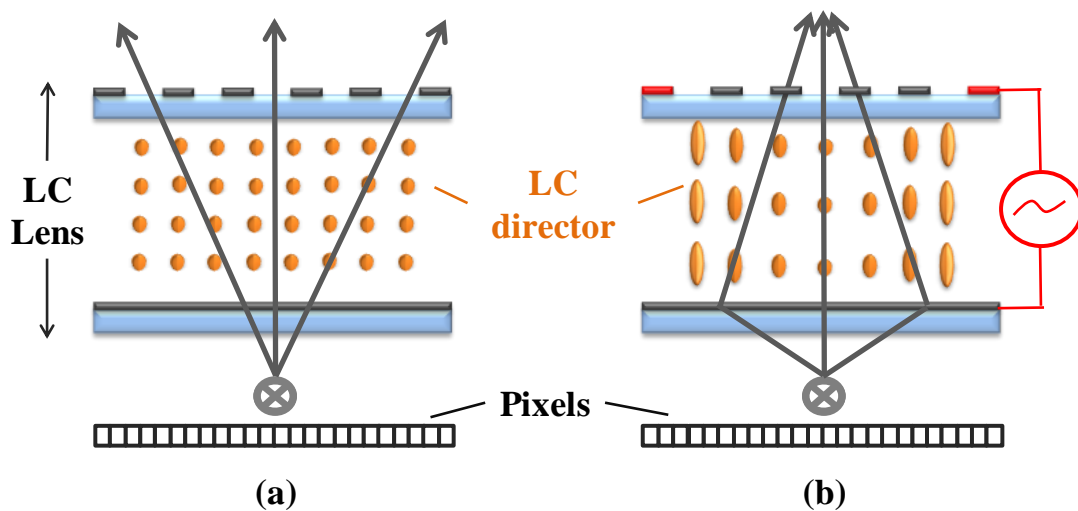
Fig. 4-1 Concept of Multi-Electrically Driven Cylindrical Liquid Crystal Lens

(MeDLC) (a) lens off state for a 2D mode and (b) lens on state for a 3D mode.

4.3 Electrode design of MeDLC

As mentioned in chapter 2, in order to achieve a lens-like distribution of LC lens. The refractive index difference must be consisted with the parabolic curve as derived in Eq.2-12. Before showing the simulation result, the simulation flow chart will be described first.

4.3.1 Simulation Steps

The simulation flow chart was formed in Fig. 4-2. First the double-electrode and multi-electrode were compared to determine the ideal Δn curve. If the double-electrode is better than multi-electrode then can begin fabrication. If not, then the most suitable electrode number for MeDLC must be found. At first we assume the electrode width to slit width ratio is 1:1. Under this condition we can found a suitable number. Third, the electrode number must be checked for suitability. In this step we use the electrode number which we just obtained, and simulate with different ratio.

Before the ratio of $W_E : W_S$ must be checked for suitability. If the ratio is not suitable

then the previous step must be repeated until the result fit all the conditions.
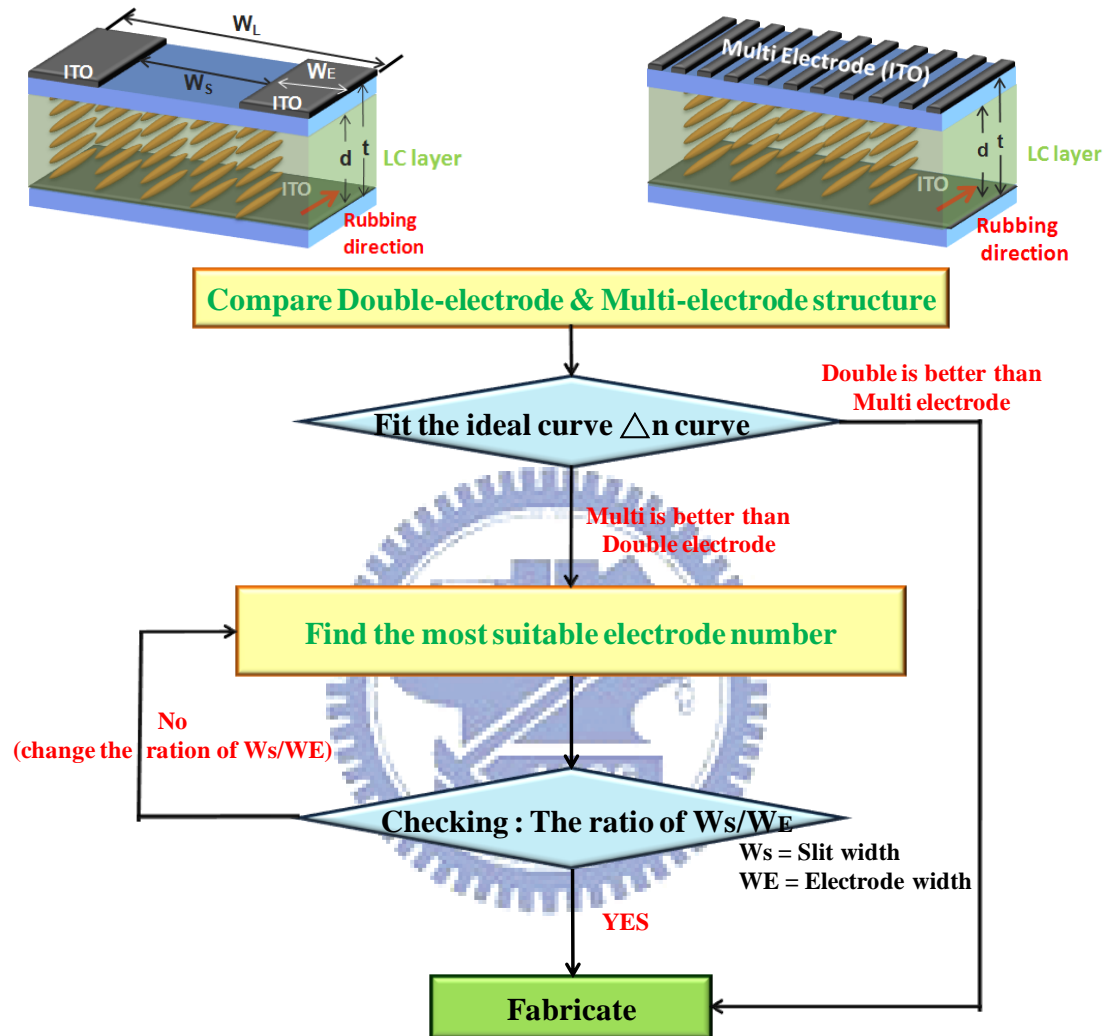

Fig. 4-2 Simulation flow chart

4.3.2 Simulation result

To investigate LC molecular orientation states in an inhomogeneous electric field [30], the commercial software DIMOS.2D (Autronic- Melchers GMBH) was used to calculate the LC director profile distribution. The LC parameters used in the simulation are as follows: nematic LC E7 (Δn = 0.22), dielectric constants $\varepsilon_\perp$ = 5.2 and ε_{ll} = 19.3, splay elastic constant K_{11} = 11.1pN, bend elastic constant K_{33} = 17.1pN, extraordinary refractive index ne = 1.7472 and ordinary refractive index no = 1.5271. The ratio of W_L / t (cell thickness t) was chosen as an optimum value which is about 2-3, where the effective area with the parabolic refractive index distribution becomes maximum [31]. Here we use a 550μm glass and lens width W_L = 1500 um . Also an error function (EF) was defined to judge the difference between the ideal curve and simulation curve, as shown in Eq.4-1.

$$EF = \sqrt{\frac{\sum_{i=i}^{aperture\_size}(S_i - P_i)^2}{aperture\_size}} *100\% \quad ....(4-1)$$

From the result of conventional double electrodes lens, a tardy changing of Δn profile was found. As the applying voltage over a certain voltage (V= 30 volt) the profile became disorderly as shown in Fig. 4-3, and that will cause aberration. That is because the slit is too wide in comparison with the lens in small voltage that electric field cannot affect the LC near the center, but in large voltage, the electric field changes between electrodes were too severe thus making the profile became disorderly. In order to keep the parabolic profile and large Δn , a multi-electrode structure is applied as shown in Fig. 4-4.
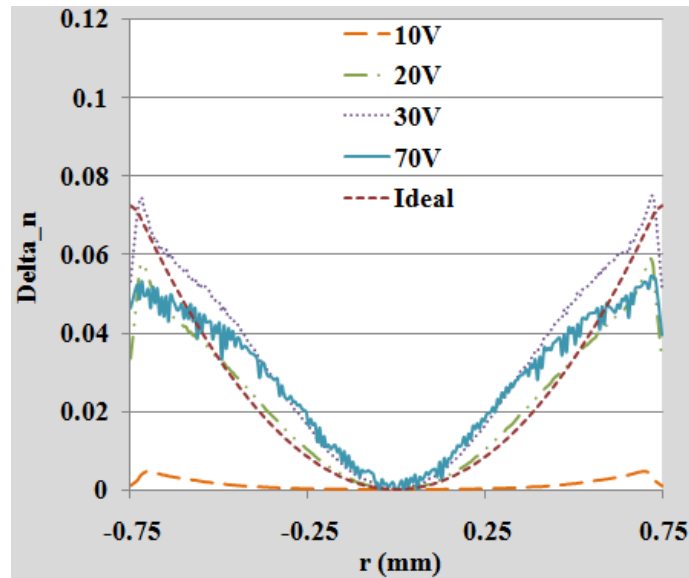
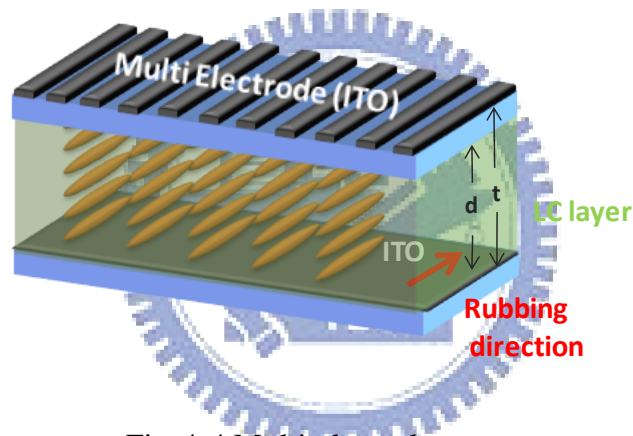Fig. 4-3 Simulation result of double electrode LC lens.

Fig. 4-4 Multi-electrode structure

By controlling the voltage to keep the Δn to be the same for each electrode number, which also means to keep in the same focal length. From the simulation result we found that seven electrodes has smaller error function, and the result tended to be saturated afterward, which the ratio of $W_E / W_S = 1:1$ as show in Fig. 4-5. And it was demonstrated that under 7 electrodes the ration of $W_E / W_S = 1:1$ is the most suitable ratio as shown in Fig. 4-6. Final, the simulation curve of our design and the cross section view of MeDLC is shown in Fig. 4-7 and Fig. 4-8. Obviously with this design the profile is more consistent with the ideal curve.
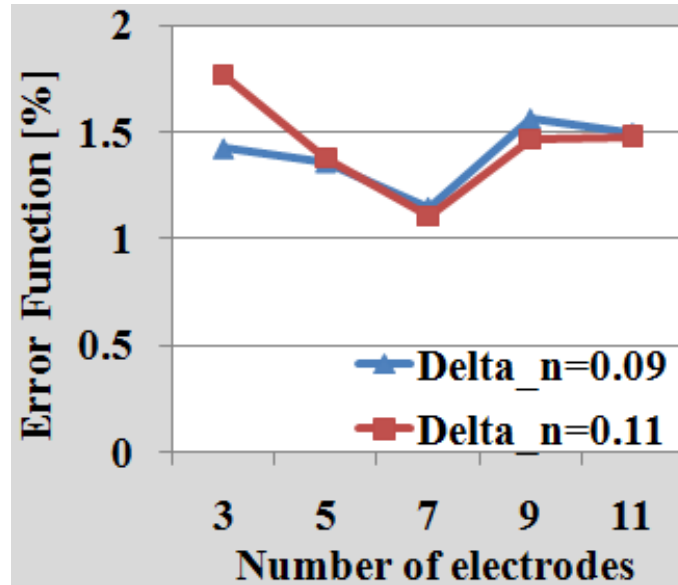
Fig. 4-5 Simulation result of error function (EF)
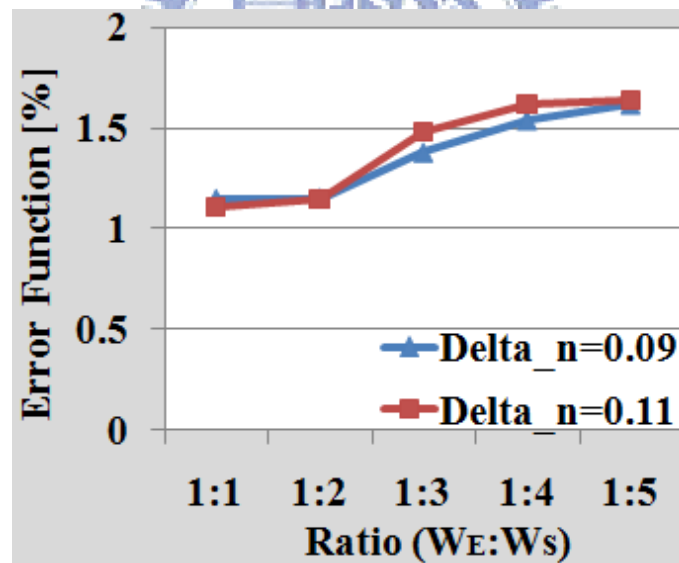
with number of electrodes

Fig. 4-6 Simulation result of error function (EF)
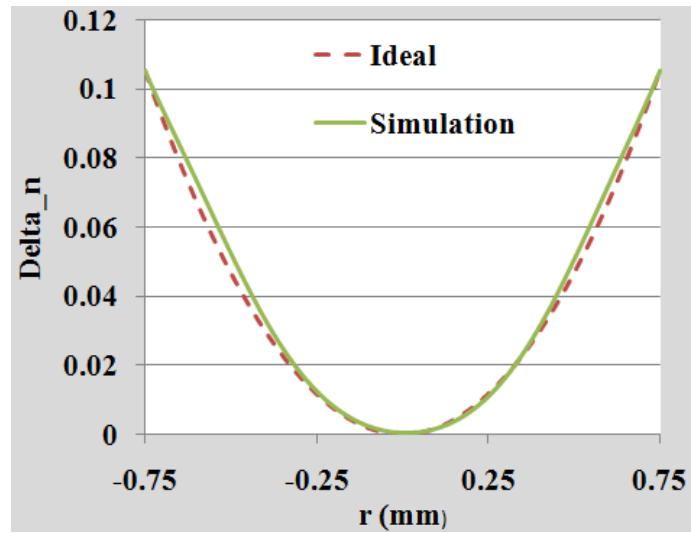
with 7 electrodes' Ratio ($W_E / W_S = 1$)
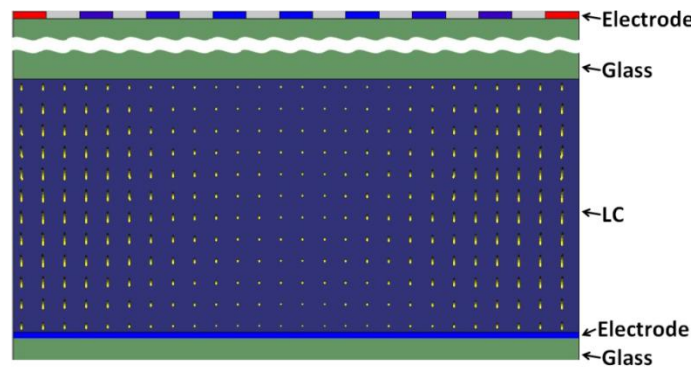
Fig. 4-7 Simulation curve of MeDLC.

Fig. 4-8 Operated cross-section of MeDLC
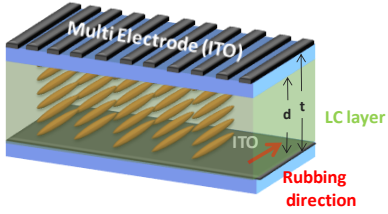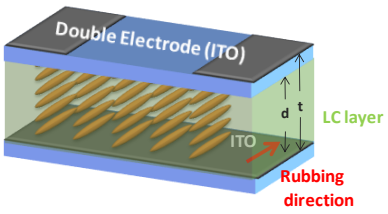
4.4 Discussion

3D displays will drastically enhance the viewing experience of future displays for many applications. Unfortunately, 3D displays generally have a lower resolution since the pixels are divided into multi view. Therefore, some 3D displays have the opportunity to switch between 2D and 3D mode such that either natural 3D images or high-resolution 2D images can be displayed.

Our task is to design a 2D/3D switchable display using liquid crystal lens with low crosstalk. Tab. 4-1 is the comparison of conventional LC lens and our novel design. The conventional liquid crystal lens suffers the issues of tardy changing of Δn. Hence can cause high crosstalk phenomenon. Therefore, the application of Multi-Electrically Driven Cylindrical Liquid Crystal Lens (MeDLC) became more serviceable.
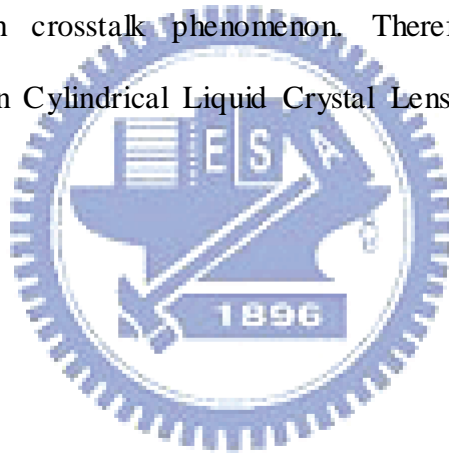
Tab. 4-1 Comparison of proposed and conventional methods.

Design	NCTU Proposed Method	Conventional Method
Δn value	O	Δ
Crosstalk	Δ	O

O: High   Δ: Low

4.5 Summary

In this section, a multi-electrode LC with closer lens-like distribution was investigated. The LC cell shows individual characteristics; that is, the refractive index distribution in conventional double electrode LC lens shows not easy to control the profile of Δn, in comparison with that of multi-electrode. Hence a simple structure with no LC alignment issue, smoother Δn curve and lower crosstalk phenomenon can be realized by MeDLC.

The MeDLC can be easily fabricated by semiconductor process. By using these well-developed fabrication processes, the designed MeDLC can be produced. The detail experimental results will be shown in next chapter.

Chapter 5

Measurement Results and Discussion

5.1 Introduction

The objective of the measurement is to investigate the phase difference in LC layer and the beam size. According to the simulation result presented in Chapter 4, and the experimental result in this chapter, our design shows great performance than conventional one. Finally, the comparison of crosstalk of MeDLC and conventional LC lens will be shown in this chapter.

5.2 Measurement results and discussion

The measurement results can be categorized into three parts: refractive index profile reconstruction, beam size and crosstalk phenomenon. The optical performance of our device can be judged with these three parts. First, our MeDLC prototype were shown in Fig. 5-1
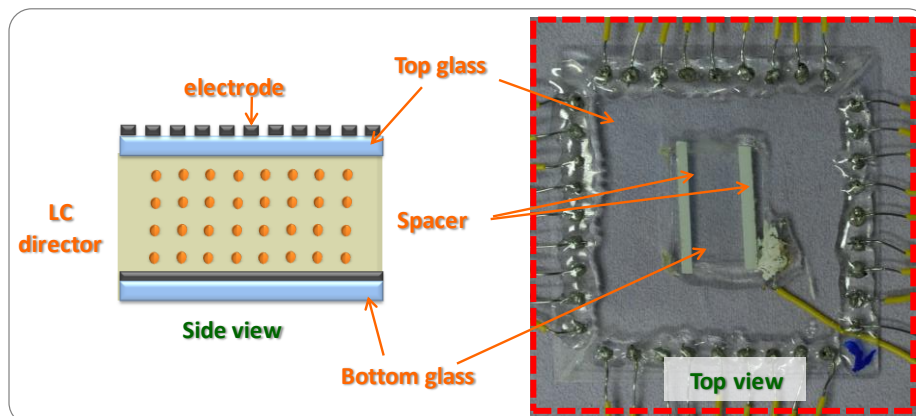

Fig. 5-1 MeDLC prototype

5.2.1 Phase profile reconstruction

From the experiment setup of crossed polarizer we can capture a series of bright and dark lines. These were caused by the phase difference in LC layer, and Δn profile can be reconstructed by calculating the spacing between the lines. Eventually, consistency with the ideal lens-like distribution will be verified, as shown in Fig. 3-7.

Refer to Fig. 5-2, shows the conventional LC lens with double electrode. We can see that the Δn curve doesn't change much with further increasing the voltage. And the curve is in a difference to the ideal curve. Therefore we can judge that the beam size of the conventional lens is large and can be expected a high crosstalk phenomenon, which will be further illustrated.
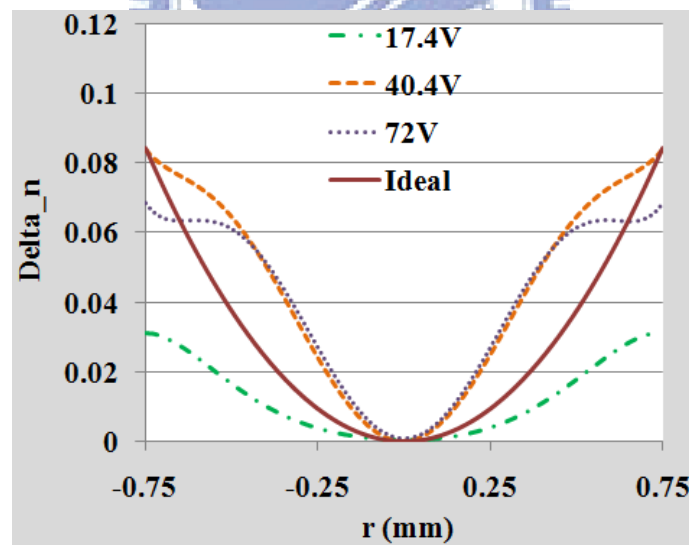

Fig. 5-2 Experimental result of double-electrode unit.

The result of seven electrodes and the ratio of $W_s : W_E = 1:1$ were shown in Fig. 5-3. First, with our design not only the full effective aperture was kept but also the curve was very consisting with the lens-like distribution. Second, is to check the suitability of the electrode number with ratio $W_s : W_E = 1:1$ as shown in Fig. 5-4. From the result seven electrodes still has the lowest error function (EF). Final, the ratio of $W_s : W_E = 1:1$ was yet found to be the most suitable ratio, as shown in Fig. 5-5. The sequence of optimized electrode value from outer electrode to center electrode is: 30v、8.6v、9.7v、0v. These measurement results were consisting with the simulation result and imply that to achieve a better performance of lens we must apply MeDLC. To be double confirmed of our design, the beam size will be illustrated at next section.
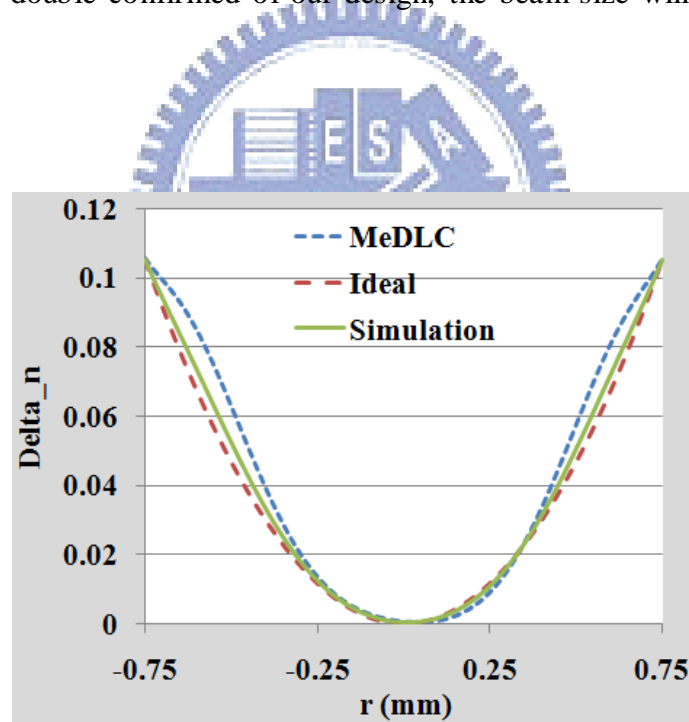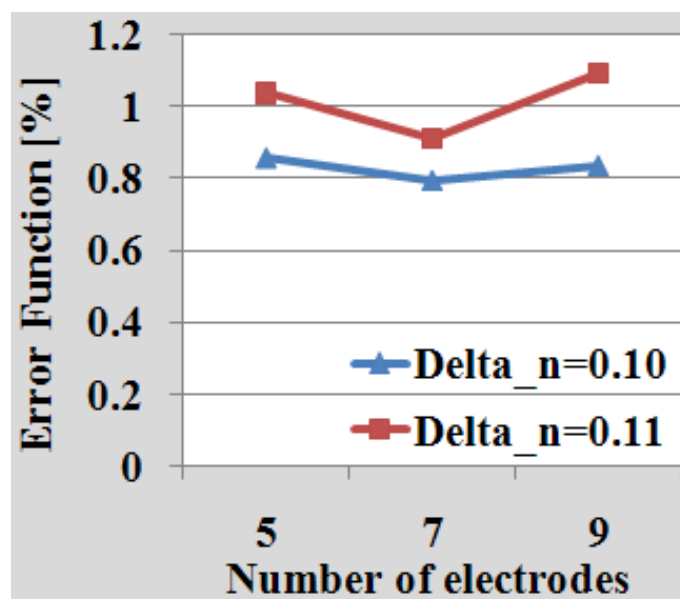

Fig. 5-3 Experimental result of MeDLC unit.
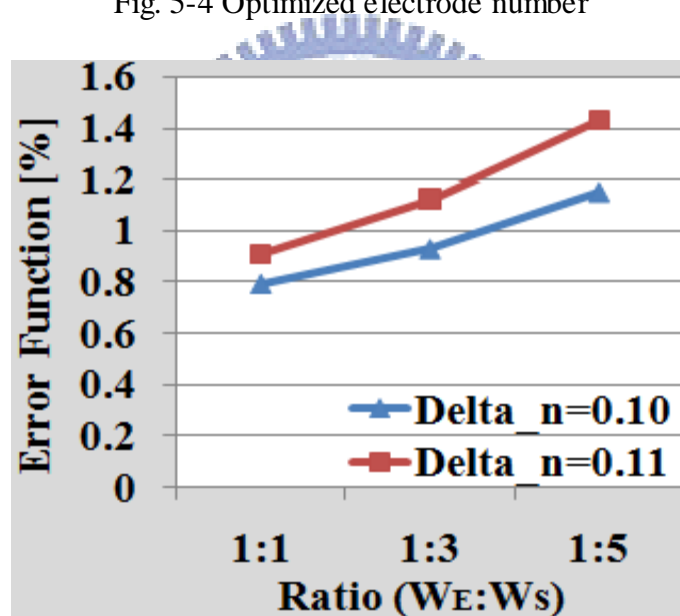
Fig. 5-4 Optimized electrode number

Fig. 5-5 Optimized $W_s : W_E$ ratio

5.2.2 Beam Size

The beam size image of the laser can be captured by CCD with polarizer parallel to the electrode direction, as shown in Fig. 3-9. The beam size was judged by the full width at half maximum (FWHM). Referring to Fig. 5-6 (a) and (b) shows the normalized intensity of conventional double electrode LC lens and the MeDLC Lens with both focal length about 3.3cm. A very sharp light peak point to the center was seen in Fig. 5-6 (b) whose beam size at full width at half-maximum is smaller than the conventional double electrode LC lens about 35%. A 2D mode can be seen after turning off the voltage, due to the laser were uninfluenced by the MeDLC as shown in Fig. 5-6 (c). These measurement results indicating a lens-like distribution was achieved and a 2D/3D switching images can be provided. Moreover, a smaller beam size can be obtained by using MeDLC lens which can result in a smaller crosstalk as well.

With this achievement, a comparison of crosstalk phenomenon of MeDLC and conventional double electrode LC lens will be demonstrated.
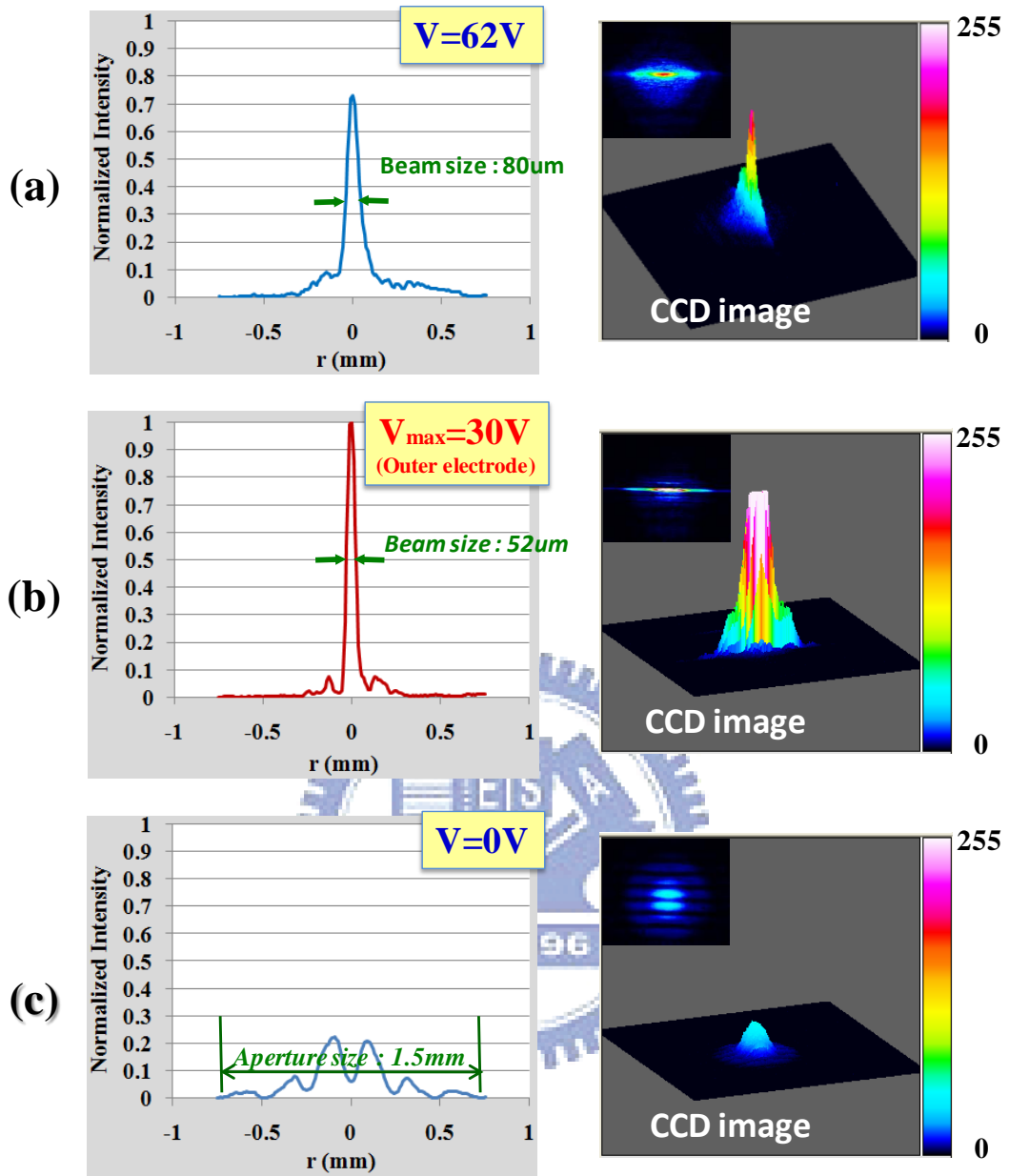
Fig. 5-6 Normalized intensity of (a) Conventional double electrode LC lens

(b) MeDLC when voltage ON (c) MeDLC when voltage OFF.

5.2.3 Crosstalk phenomenon

In the context of 3D displays, crosstalk is the amount of left image that leaks into the right view and right image that leaks into the left. When the crosstalk is too high, the brain no longer perceives two different viewpoints and therefore no disparity.

To investigate the crosstalk, the commercial software Light-Tools was used to calculate the crosstalk phenomenon of MeDLC and conventional double electrode LC lens by inputting the Δd profile. Δd is the height of the lens and is substituted by Δn as shown in Eq.5-1, and Eq.5-2. The definition of crosstalk was shown in Eq.2-13 [19].

$$\Delta n_{LC} \cdot d_{LC} = n_{lens} \cdot \Delta d_{lens} \quad\text{...} \quad (5\text{-}1)$$

$$\Delta d_{lens} = \frac{\Delta n_{LC} \cdot d_{LC}}{n_{lens}} \quad\text{...} \quad (5\text{-}2)$$

By using ray-tracing, the crosstalk of each viewing zone was simulated. A light intensity distribution of each pixel can be obtained by shifting the light source from pixel 1 to pixel 9 at a time. For the eye distance of 65mm and a 9m viewing distance, the crosstalk phenomenon based on conventional lens and proposed design were shown in Fig. 5-7 and Fig. 5-8. The results demonstrate that 3D display with proposed design has less crosstalk than the conventional one about 43% as shown in Tab. 5-1. Therefore, the image quality of each viewing zone can be improved due to lower cross talk.
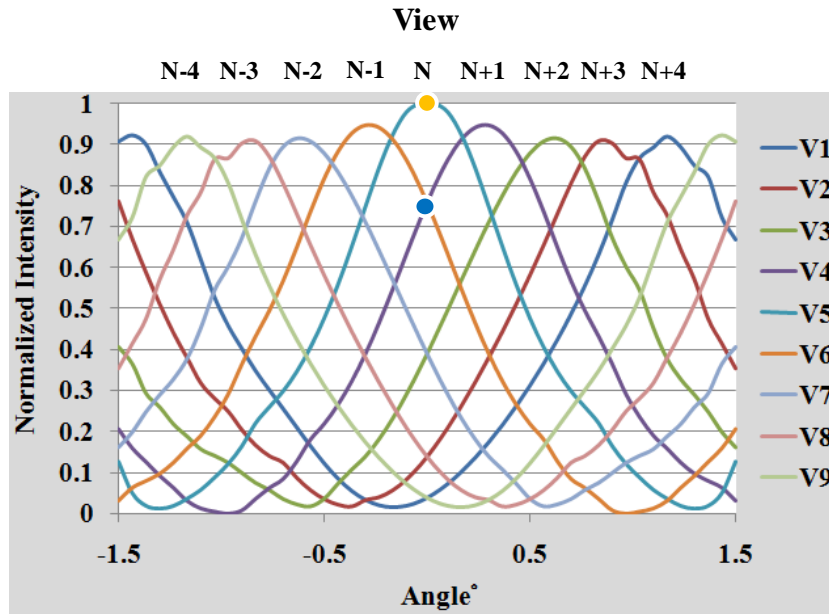
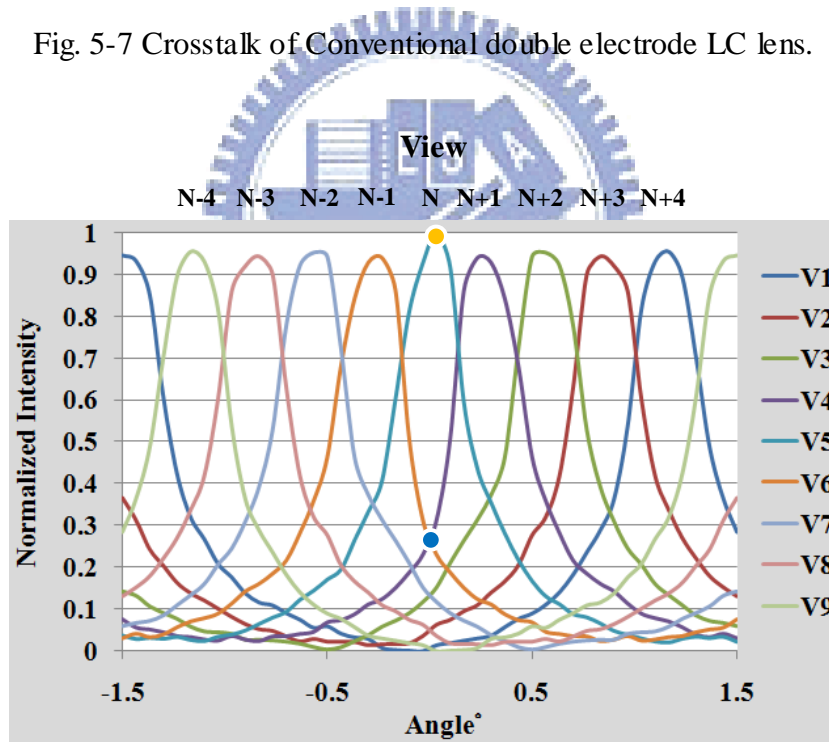Fig. 5-7 Crosstalk of Conventional double electrode LC lens.

Fig. 5-8 Crosstalk of MeDLC

Tab. 5-1 Crosstalk was simulated by Light-Tools

	MeDLC	Conventional Double Electrode
Crosstalk (%)	~24	~42

5.3 Numerical Aperture vs. Operation Voltage

To judge the operation voltage, we take the numerical aperture (NA) into account as shown in Eq.5-3, where *n* is the index of refraction of the medium in which the lens is working and D is the diameter of the lens. Here our aperture is 1508um. With same numerical aperture a lower operation voltage was obtained by using MeDLC Lens because it can control the liquid crystal profile by each segment electrode. The numerical aperture with same operation voltage of multi-electrode and double electrode lens were compare as well. From the result the multi-electrode is higher than the double electrode and that means it has higher optical power to banded or focus the light of 3D display. And the numerical aperture is about a factor of 1.66 higher than the double electrode as shown in Fig. 5-9. Therefore, a better optical power as a cylindrical lens and lower operation voltage was indicated. The crosstalk phenomenon can be described by numerical aperture as well. A small numerical aperture can also mean a large focal length; in this case the effect of crosstalk can be serious due to a close image of left and right as shown in Fig. 5-10 (a). As for the large numerical aperture which result in a small focal length can separate the image of both eyes widely, therefore can have a lower crosstalk phenomenon.

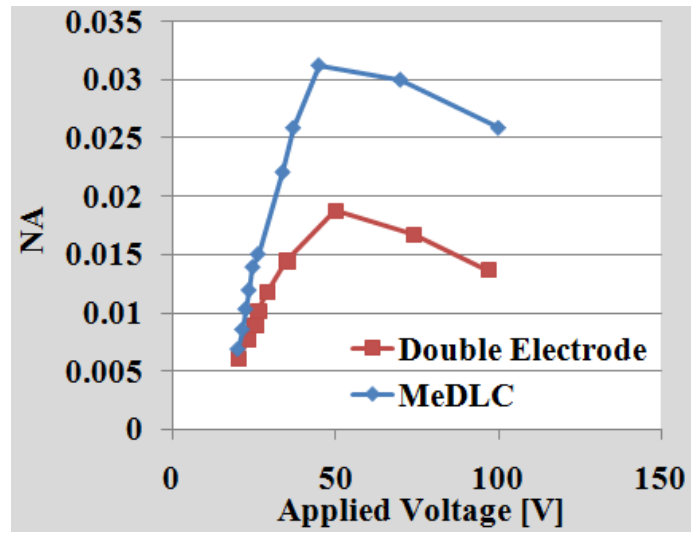$$NA = n \sin \theta = n \sin \tan' \frac{D}{2f} \cong n \frac{D}{2f}$$ …………………………………(5-3)
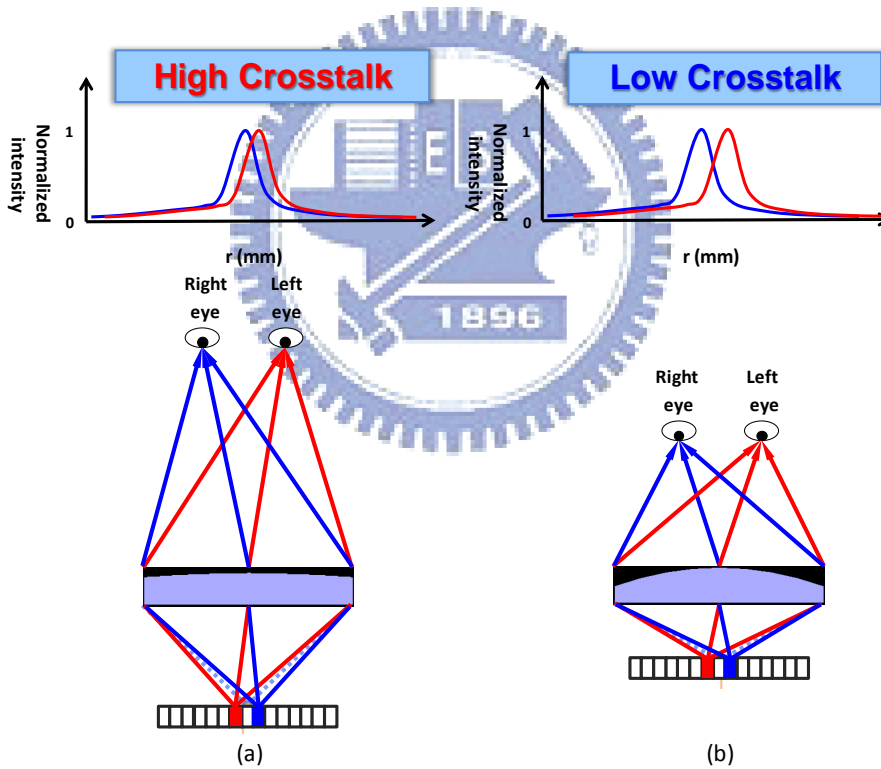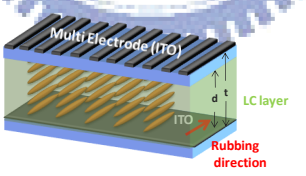
Fig. 5-9 Numerical Aperture property
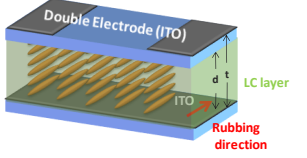
Fig. 5-10 The crosstalk of (a) small numerical aperture (b) large numerical aperture.

5.4 Summary

For the lens-like distribution, beam size, crosstalk, numerical aperture and operation voltage of conventional double electrode LC lens and proposed design MeDLC are summarized in Tab. 5-2. The beam size is reduced by 35% and the crosstalk with proposed MeDLC is lower about 43%. Furthermore the operation voltage of MeDLC Lens is lower than the double electrode lens and have a numerical aperture improves by 66%. In addition, the results indicate that the 2D/3D switching display with proposed method not only smaller beam size and lower crosstalk, but lower operation voltage.

Tab. 5-2 Comparison of conventional and proposed MeDLC.

Design	NCTU Proposed Method	Conventional Method
Beam Size Decrease Factor	x0.65	1
Crosstalk (%)	~24	~42
Numerical Aperture Increase Factor	x1.66	1
Operation voltage	O	Δ

Δ: High   O: Low

Chapter 6

Conclusions and Future Work

6.1 Conclusions
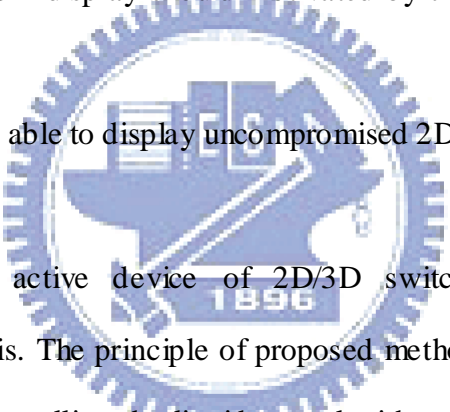
In our opinion a viable 3D display should fulfill the following requirements:

1. The display should be auto-stereoscopic. It should allow freedom of movement with multi viewer potential.

2. The development of 3D display should motivated by trying to realize the image appears more natural.

3. The display should be able to display uncompromised 2D content.

Therefore, a novel active device of 2D/3D switching display has been demonstrated in this thesis. The principle of proposed method is to produce a natural 2D and 3D images by controlling the liquid crystal with switching ON and OFF the voltage. The simulation results indicate that a closer lens-like distribution can be achieved by our device. The measurement result also indicates that our device can be closer to the ideal lens-like distribution. And the numerical aperture (NA) of our device shows an improve by a factor of 1.66 which can result in a smaller volume of display and smaller crosstalk. Also the voltage requirement is much lower with same NA. In addition, due to a smaller beam size of proposed design the crosstalk of our device is lower than that of the conventional double electrode LC lens about 43%. In conclusion, the 3D displays with proposed method not only smaller beam size and lower crosstalk, but lower operation voltage.

The proposed design can also be applied for combining with a head tracking device. By tracking the position of the head and a LC lens which is able to move horizontally with respect to the viewer position. Therefore, a freedom of movement with wide viewing angle and high resolution 3D images can be perceived.

6.2 Future work

Currently although our operation voltage is lower than that of the conventional double electrode LC lens (current operation voltage of MeDLC lens is about 30 volt). Nevertheless we think this is not lower enough due to a thick glass substrate (550um) between the electrodes and liquid crystal. In order to further reduce the operation voltage the thickness of the substrate between the electrodes and liquid crystal lens must be reduced as shown in Fig. 6-1. And our task in the future is to study and find a suitable thickness and parameter (ε: dielectric property) of a dielectric layer. And with more electrodes to control the lens-like profile which will also be an optimized design.
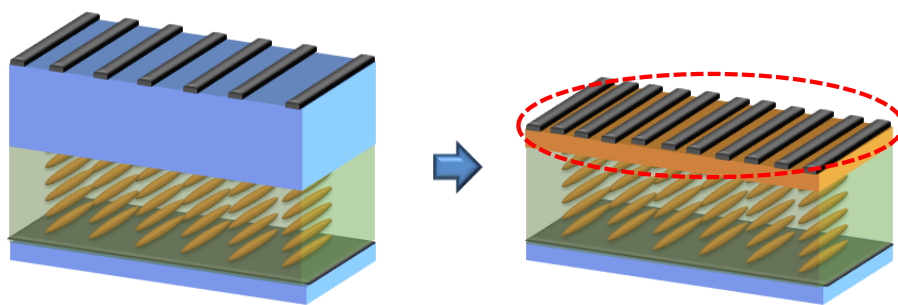

Fig. 6-1 Reduce the operation the voltage by reduce the substrate thickness with an optimized parameter and structure design.

Also from calculating the intensity distribution of MeDLC and without MeDLC when off state as shown in Fig. 6-2. The intensity distribution with MeDLC shows a diffraction pattern from ITO. This will reduce the image quality in displaying 2D images. To overcome this problem is to coating a material which has the same absorption and refraction rate corresponding to the ITO. In this case the phenomenon of diffraction can be reduce and without losing the quality in 2D mode. Therefore we will further study about this kind of material in the future.
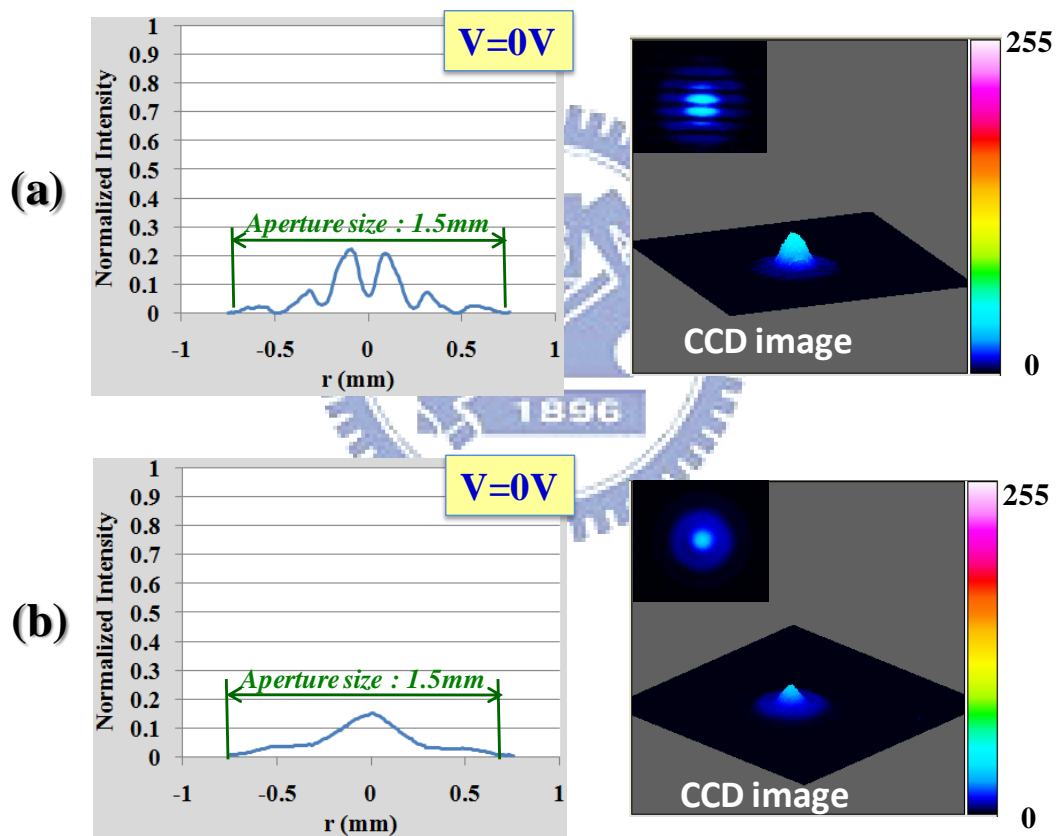

Fig. 6-2 without driving voltage (a) MeDLC (b) without ITO pattern

Beside the issue of operation voltage and diffraction in off state. In this research even though the crosstalk can reduced to 24% only. However, the effect of crosstalk in multi-view autosterescopic 3D displays has been reported that the tolerance limit of visual comfort is around 10% [34]. Therefore our second task is to reduce the crosstalk to about 10%. At previous chapter we have described the relative between the focal length and crosstalk. Fig. 6-3 shows a simulation of the trend of the crosstalk versus focal length. From the result, in order to achieve a 10% crosstalk our focal length needs to be reduced to about 1.9cm. And this can be resolved by larger the cell gap or change a liquid crystal which has high Δn.
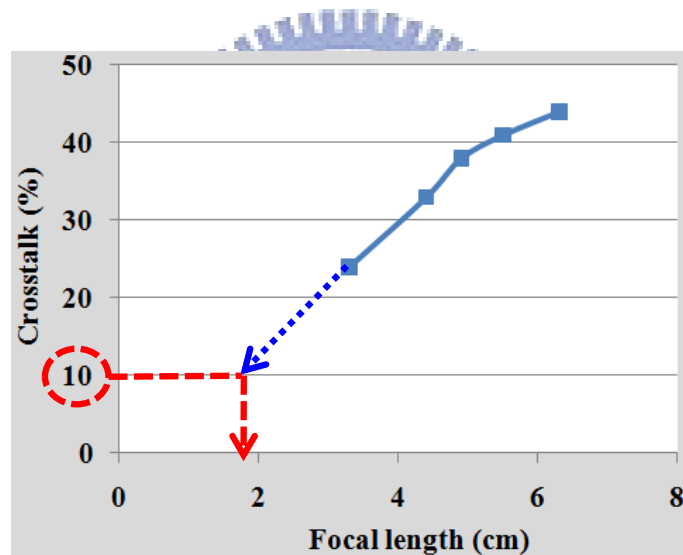

Fig. 6-3 Crosstalk vs. focal length

Reference

[1] J. Mansson, "Stereovision: A model of human stereopsis," Lund Univ. *Congnitive Science, Tech. Rep.*, (1998)

[2] E. Edirisinghe, J.Jiang, "Stereo image, an emerging technology". *SSGRR*, L'Aquila,Italy, (2000)

[3] L. Hill, A. Jacobs "Invited paper: 3-D Liguid Crystal Displays and Their Applications" *IEEE* Vol. 94, No. 3, March (2006)

[4] J. S. Kollin, S. A. Benton, M. L. Jepsen,"Real-Time Display of 3-D Computed Holograms by Scanning the Image of an Acoustic-Optic Modulator," *SPIE Proceedings*, Vol. 1212, pp.174 (1990)

[5] "Laser Based 3D Volumetric Display System," *US Patent* No.5,854,613 (1998)

[6] K. Toyooka, T. Miyashita, T. Uchida, *Proc. SID'01*, pp.174 (2001).

[7] T. Sasagawa, A. Yuuki, S. Tahata, O. Murakami, K. Oda, "Dual Directional Backlight for Stereoscopic LCD", *Proc. SID'03*, pp.399 (2003).

[8] Y. M. Chu, K. W. Chien, H. P. D. Shieh, J. M. Chang, A. Hu, Y. C. Shiu, and V. Yang, *J. Soc. Inf. Display,* No.13, pp.875 (2005).

[9] K. W. Chien and H. P. D. Shieh, *Appl. Opt*., No.45, pp.3106 (2006).

[10] L. Lipton et al., *Proc. SPIE*, No.4660, pp.229 (2002).

[11] G. Woodgate, J.Harrold, A. Jacobs, etc., "Flat panel autostereoscopic displays-characterization and enhancement", *Proc. SPIE, Stereoscopic Displays and Virtual Reality Systems VII,* vol. 3957, pp.153-164, Apr. (2000).

[12] D. Takemori, K. Kanatami, S. Kishimoto, S. Yoshi, and H. Kanayama, *Proc. SID'95*, pp.55 (1995).

[13] H. Morishima, H. Nose, etc., "Rear cross lenticular 3D display without eyeglasses", *Proc. SPIE, Stereoscopic Displays and Virtual Reality Systems VII*, vol.3295, pp.193-202, Apr. (1998).

[14] Cees van Berkel and John A Clarke. "Characteisation and optimization of 3D-LCD module design", *Proc. SPIE*, Vol.3012, pp.179-187 (1997)

[15] J. Young, B. Javidi, "Three-dimensional image methods based on multiview images", *J. Display. Tech.*, Vol. 1, pp.125-140, (2005).

[16] H. Isono et al. *Japanese Pat*. Appln.JP03-119889, (1991)

[17] M.G.H Hiddink, S.T. de Zwart, etc. "20.1: Locally switchable 3D displays", *SID* pp.1142-1145 (2006)

[18] W.L. IJzerman, S.T. de Zwart, T. Dekker, "Design of 2D/3D switchable displays", *SID*, pp.98-101, (2005)

[19] Hyung-ki Hong, Sung-min Jung, etc. "25.3: Autostereoscopic 2D/3D switching display using electric-field-driven LC lens (ELC Lens)", *SID* pp.348-351 (2008)

[20] G.J. Woodgate, J. Harrold, "A new architecture for high resolution autostereoscopic 2D/3D displays using free-standing liquid crystal microlenses", *SID*, pp.378-381, (2005)

[21] G.J. Woodgate, J. Harrold, "Key design issues for autostereoscopic 2D/3D displays", *Euro. Display*, pp.1-4, 10 September (2005)

[22] S.J. Battersby, "Auto-stereoscopic Display Apparatus", US6069650, (2000).

[23] G.J. Woodgate, J. Harrold, "LP.1:High Efficiency Reconfigurable 2D/3D Autostereoscopic Display", *SID Digest* (2003)

[24] Stephen T. Kowel, Dennis S. Cleverly and Philipp G. Kornreich, "Focusing by electrical modulation of refraction in a liquid crystal cell.", *Applied Optics*, Vol.23, No.2, pp.278-289 (1984)

[25] P. Yeh and C. Gu, Optics of Liquid Crystal Displays, Chapter 4, J. *Wiley and Sons*, New York (1999)

[26] GRINTECH, http://www.grintech.de

[27] E. Hecht, Optics (Forth Edition), *Addison Wesley* (2002).

[28] H. REN, Y.H. FAN, et al. "Tunable-Focus Cylindrical Liquid Crystal Lens", *Jpn. J. Appl. Phys*. Vol. 43 pp.652 (2004)

[29] E.J.A. Brouwer, "Frequency analysis on a 3D display", *Koninklijke Philips Electronics N.V*., Technical note PR-TN 2005/00947, (2004)

[30] Y.H. LIN, at el. "Tunable-Focus Cylindrical Liquid Crystal Lenses", *Jpn. J. Appl. Phys*. Vol. 44, No. 1, pp.243-244,(2005)

[31] S. SATO, "Applications of Liquid Cristal to Variable-Focusing Lenses", *Opt. Re*. Vol.6, No. 6, pp.471-475 (1999)

[32] Y.P. Huang, C.W. Chen, T.C. Shen, "Invited paper: High resolution autostereoscopic 3D display with scanning multi-electrode driving liquid crystal (MeDLC) lens", *SID*, pp.336-339, (2009)

[33] T.C. Shen, L.Y. Liao, C.W. Chen, Y.P. Huang, H.P. Shieh, "Autostereoscopic 2D-3D display with multi electrically driven cylindrical liquid crystal lens", *OPT*, (2009)

[34] T. Jarvenpaa, M. Salmimaa, "Optical characterization of autostereoscopic", J.

SID, pp.825-833, (2008)